CHAPTER III
RESULTS AND DISCUSSION

3. Results and discussion

3.1 Extraction of 6-deoxyclitoriacetal from the dried roots of *Stemona collinsae* Craib.

6-deoxyclitoriacetal (**1**) and stemonal (**2**) were obtained as colorless and yellow needles, respectively. Its melting point, IR, NMR and MS data are in agreement with those reported in the literatures [50, 51].

The crystal structure of **1** was reported [9]. The structure composed of four fused ring A, B, C and D. The molecule has a bent-shaped conformation at C6a to C12a [Fig. 7]. Whereas, the crystal structure of **2** [Table 1] has the similar structure with **1**, it has a planar structure. The structure of **2** [A1] composed of four fused ring A, B, C and D (Fig. 7). Planar plane AB and CD of **2** are similar to that of **1**. Both **1** and **2** are significantly different in the central ring B and C (C6a to C12a). Crystal structure of **1** adopts a roof-shaped conformation while **2** show a planar conformation.

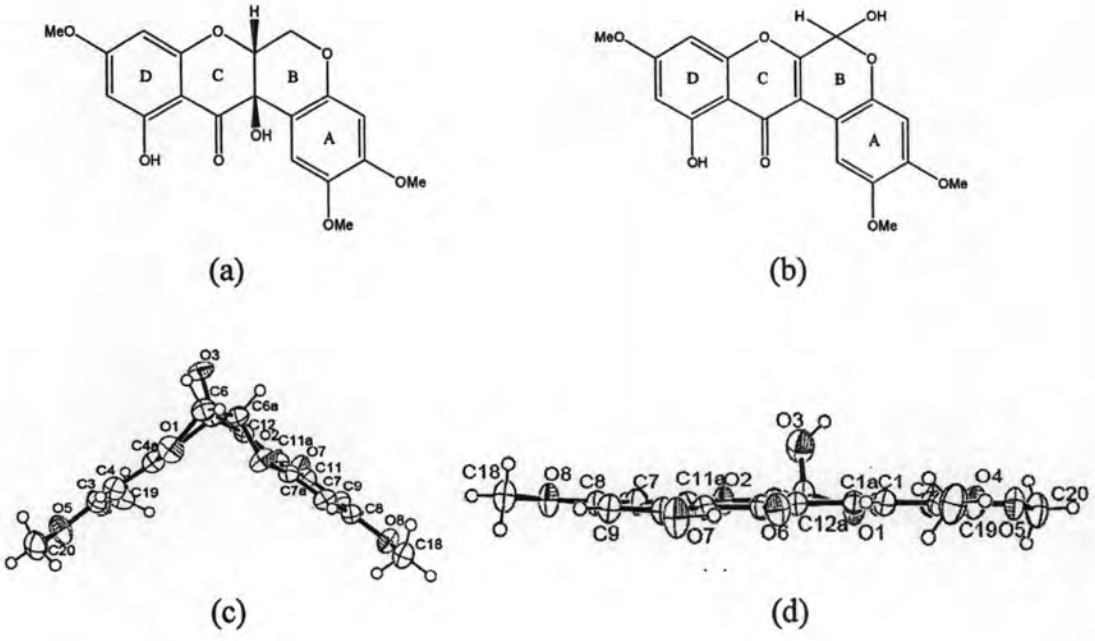

Fig. 7 Chemical structure of (a) 6-deoxyclitoriacetal, (b) stemonal, ORTEP structure showed top view of (c) 6-deoxyclitoriacetal and (d) stemonal.

Table 1 Crystal data and summary of data collection and structure refinement of **1** and **2**

Crystal data	**1**	**2**
Compound	$C_{19}H_{18}O_8$	$C_{19}H_{16}O_8$
CCDC-No.	1267/980	1260/113
Wavelength	Mo K_α radiation (0.71073 Å)	Mo K_α radiation (0.71073 Å)
Diffraction	Bruker SMART CCD	Enraf-Nonius CAD
Colour	Colorless needle	Yellow needle
size	0.30x0.30x0.63	0.25x0.30x0.50
Fw	374.32	372.32
Crystal system	Orthorhombic	Triclinic
Space group	$P2_12_12_1$	$P(-1)$
Z	4	2
a, b, c (Å)	6.3960(3), 15.3916(4), 17.1953(8)	8.1820(5), 9.7430(6), 10.8700(8)
α, β, γ (°)		77.071(4), 76.651(4), 76.545(4)
μ (cm^{-1})	1.16	1.21
Cell volume ($Å^3$)	1692.8	806.63(9)
*N(hkl)*measured,	12600, 4859	5440, 3231
*N(hkl)*unique	317	388
$N(param)_{refined}$	SHELXS-97, SHELX-97,	SIR-97, SHELX-97,
Programs	ORTEP-3	ORTEP-3
Final *R* indices [$I>2\sigma(I)$]	$R1 = 0.042$, $wR2 = 0.097$	$R1 = 0.073$, $wR2 = 0.203$

3.2 Cytotoxic activities of obtained rotenoid compounds

Both **1** and **2** were studied in cytotoxicity against various types of human carcinoma, such as KB (Human mouth carcinoma), BC (Breast cancer), NCL-H187 (Human small lung cancer) respectively (Table 2).

Table 2 Cytotoxic activities of 6-deoxyclitoriacetal (**1**) and stemonal (**2**)

Compound	**Anti-KB** IC_{50} **(μg/ml)**	**Anti-MCF7** IC_{50} **(μg/ml)**	**Anti-NCl-H187** IC_{50} **(μg/ml)**
Doxorubicin HCl	0.16±0.05	0.11±0.02	0.03±0.01
6-deoxyclitoriacetal	0.08	0.26	0.04
stemoanl	Inactive	Inactive	Inactive

KB, MCF7 and NCI-H187 are oral cavity cancer, breast cancer and small cell lung cancer, respectively.

The results of anticancer activity assays showed that **1** had good anticancer activities on three types of human carcinoma when compared with doxorubicin HCl as a positive control. A comparison between **1** and doxorubicin HCl showed that both compounds had similar parts of molecular moieties (Fig. 8). It was reported that doxorubicin HCl had a planar polycyclic aromatic part that intercalated into the space between two adjacent base pairs of DNA and inhibited the transcription and replication processes. **1** also had a planar part that may intercalate into DNA as well. Stemonal (**2**) is a rotenoid compound with a planar shape. It also had a planar part and the similarity between molecule structures of **1** and **2** (Fig. 7) is more obvious than that of **1** and doxorubicin HCl (Fig. 8). However, **2** had no anticancer activity.

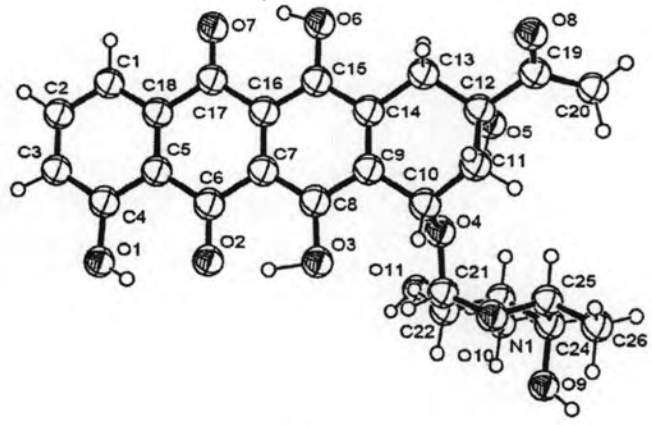

(a)

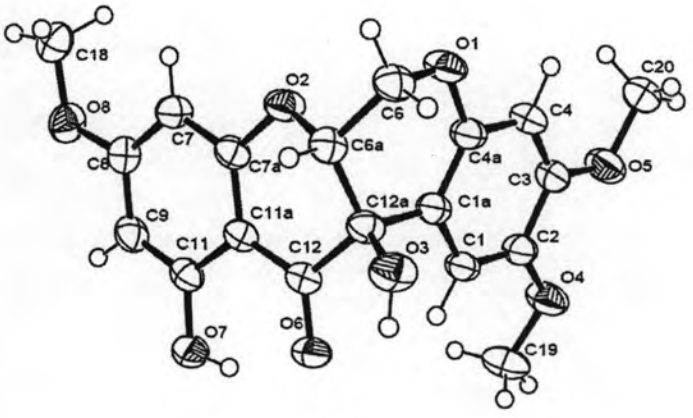

(b)

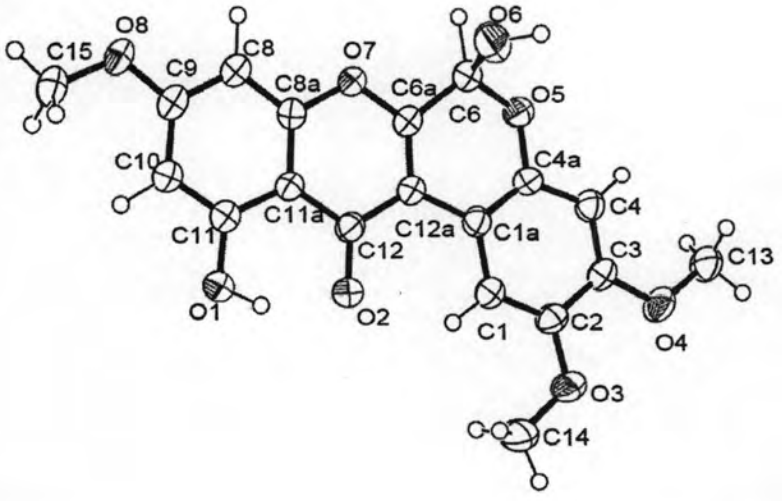

Fig. 8 ORTEP drawing of (a) doxorubicin HCl, (b) **1**, (c) **2** showing 50 % probability displacement ellipsoids

A possible explanation for their differences in anticancer activities lied in their geometries (Table 3). The only difference between molecular structures of **1** and **2** was at the position of C6a-C12a. The single bond at C6a-C12a in **1** caused its bent shape and the double bond at the same position in **2** caused its planar shape.

Table 3 Compared structure of doxorubicin HCl, **1** and **2**

doxorubicin HCl	**1**	**2**
1. Present a planar part in aglycone part (ring B, C and D) 2. Present a bent shape at the amino sugar position 3. Hydrogen bonding at N3 of the amino sugar with base CpG in the minor groove of DNA	1. Present a planar part in ring (A, B) and ring (C, D) 2. Present a bent shape at C6a-C12a between ring B and C 3. Hydrogen bonding at hydroxyl group (C11)	1. Present planar molecule moiety at ring (A, B, C and D)

3.3 Drug-DNA binding studies

3.3.1 Spectral measurements

3.3.1.1 UV-titration experiments

The binding ability of **1** and **2** with calf thymus DNA were studied using UV-via spectroscopy to observe the changing spectrum of **1** and **2** when binding with calf thymus. The concentration of **1** and **2** were determined by spectrophotometry at 295 nm using a molar extinction coefficient of 24,615 and 21,428 M^{-1} cm^{-1} respectively. The spectrum of **1** and **2** and calf thymus DNA were shown in Fig 9 and 10, respectively.

The absorption spectrum of **1** and **2** were changed from 295 to 290 nm in **1** and 294 to 290 nm in **2** after mixing with calf thymus DNA. These revealed the shifted spectra about 1.69 % in **1** and 1.32 % in **2**. Both **1** and **2** presented the hyperchromism, indicating that **1** and **2** can form a complex with double-helical DNA and evaluate the structural changes in the DNA helix.

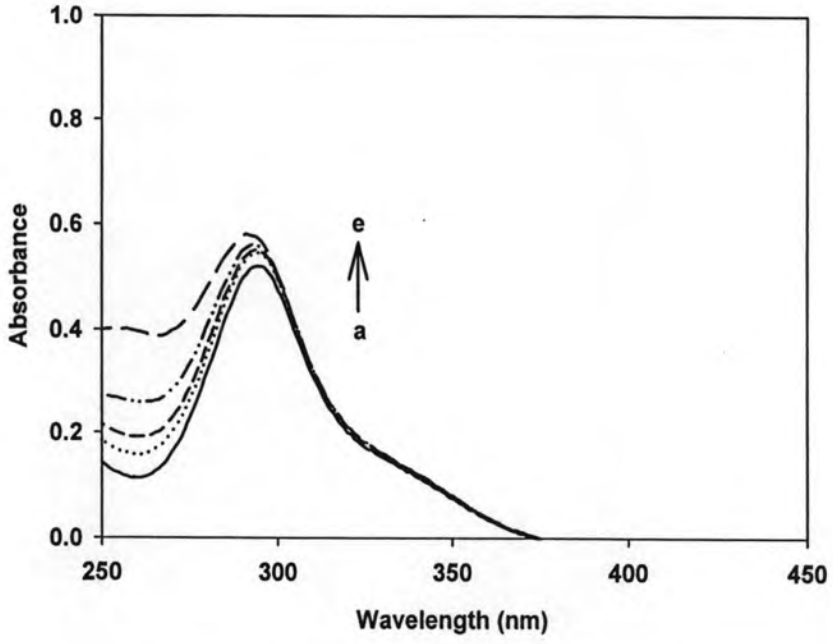

Fig. 9 Absorption spectra of **1** (2.5 x 10^{-5} M) in the absence and presence of calf thymus-DNA (x 10^{-4} M): a, 0.0; b, 1.1; c, 2.2; d, 4.5; e, 6.7 in phosphate buffer pH 7.0. Arrow shows that the absorbance changes upon increasing DNA concentration.

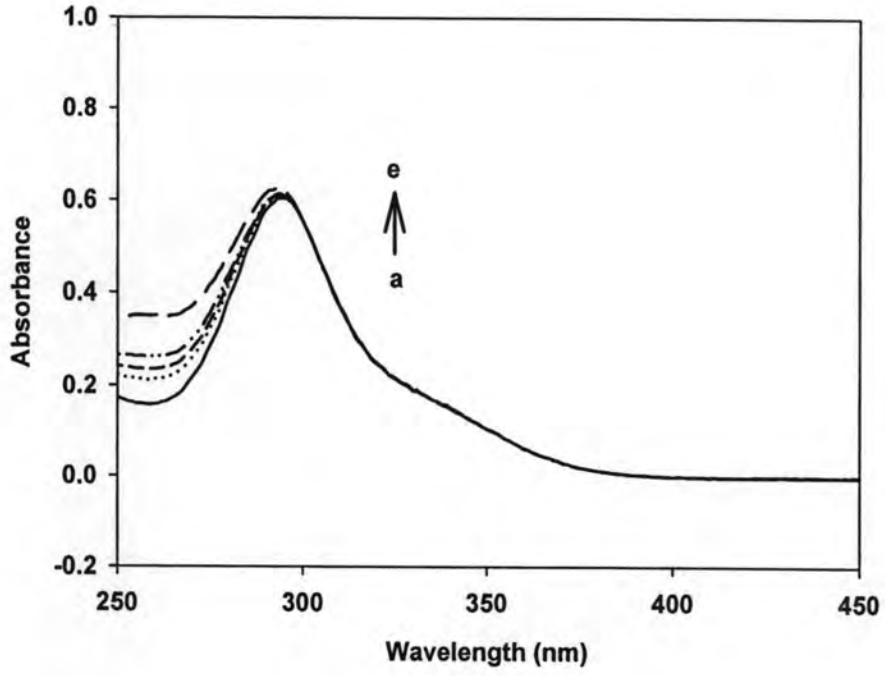

Fig. 10 Absorption spectra of **2** (2.8 x 10^{-5} M) in the absence and presence of calf thymus-DNA (x 10^{-4} M): a, 0.0; b, 1.1; c, 2.2; d, 4.5; e, 6.7 in phosphate buffer pH 7.0. Arrow shows that the absorbance changes upon increasing DNA concentration.

3.3.1.2 DNA melting studies

To gain further insight into the binding ability of **1** and **2** into the helix, DNA melting studies were monitored by following the UV absorbance of the ct-DNA at 260 nm as a function of temperature, in the absence or presence of **1** and **2**. The melting profiles of ct-DNA and its complexes with **1** and **2** are shown in Fig. 11. The melting temperature (T_m) of ct-DNA alone is at 67.8°C whereas for the ct-DNA with **1** complex the T_m is at 72.6°C, showing a 4.8°C increase in the transition temperature of ct-DNA. On the other hand, it is seen from Fig. 11 that the T_m changes from 67.8°C (ct-DNA alone) to 70.0°C on complexation with **2**, showing a 2.2°C increase in the transition temperature of ct-DNA. Changes in absorbance (dA) with respect to increasing temperature (dT) at 260 nm for ct-DNA and the ct-DNA with **1** and **2** showed in Fig 12.

The experiment data from DNA-melting studies revealed that **1** and **2** stabilizes the DNA helix and that the melting temperature (T_m) of DNA is increased 4.8°C in **1** and 2.2°C in **2**. The results of T_m showed that both **1** and **2** could intercalate into DNA base pairs, but **2** could not form a stable binding **2**-DNA complex, probably because **2** could not strongly bind with DNA, or due to the presence of the –OH (C6) above the molecular plane, causing the steric hindrance that prevented its insertion into the DNA strand. In contrast, C11-OH of **1** is hydrogen-bonded to base pairs at the minor or major grooves in DNA. Interestingly, doxorubicin HCl also presents a bent shape and H-bonding with DNA. Therefore, both characteristics contributed to anti-cancer activities of **1** and doxorubicin HCl

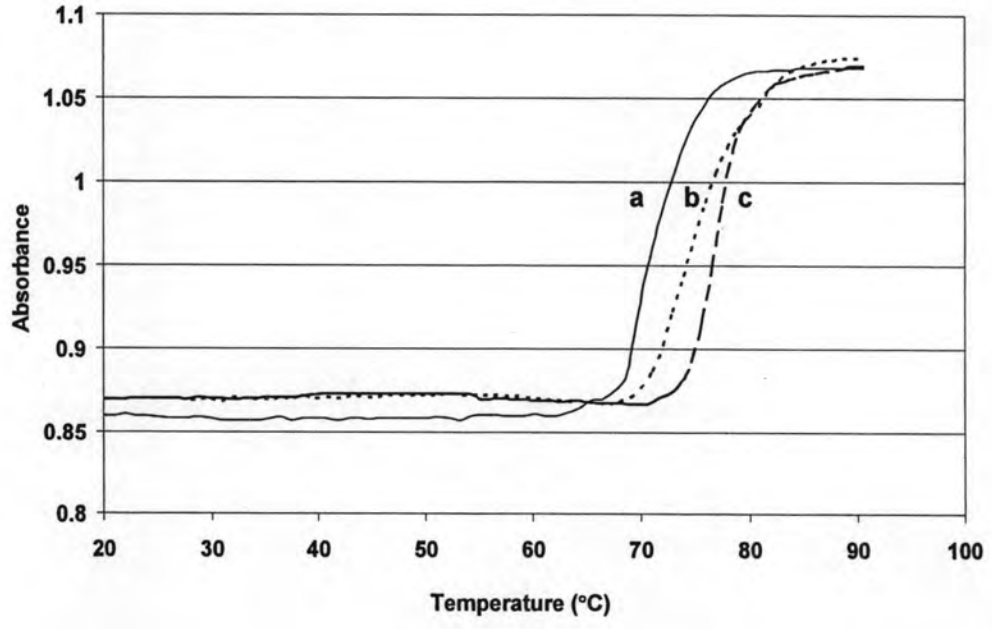

Fig. 11 Melting profiles of (a) ct-DNA, (b) ct-DNA with **2** and (c) ct-DNA with **1**

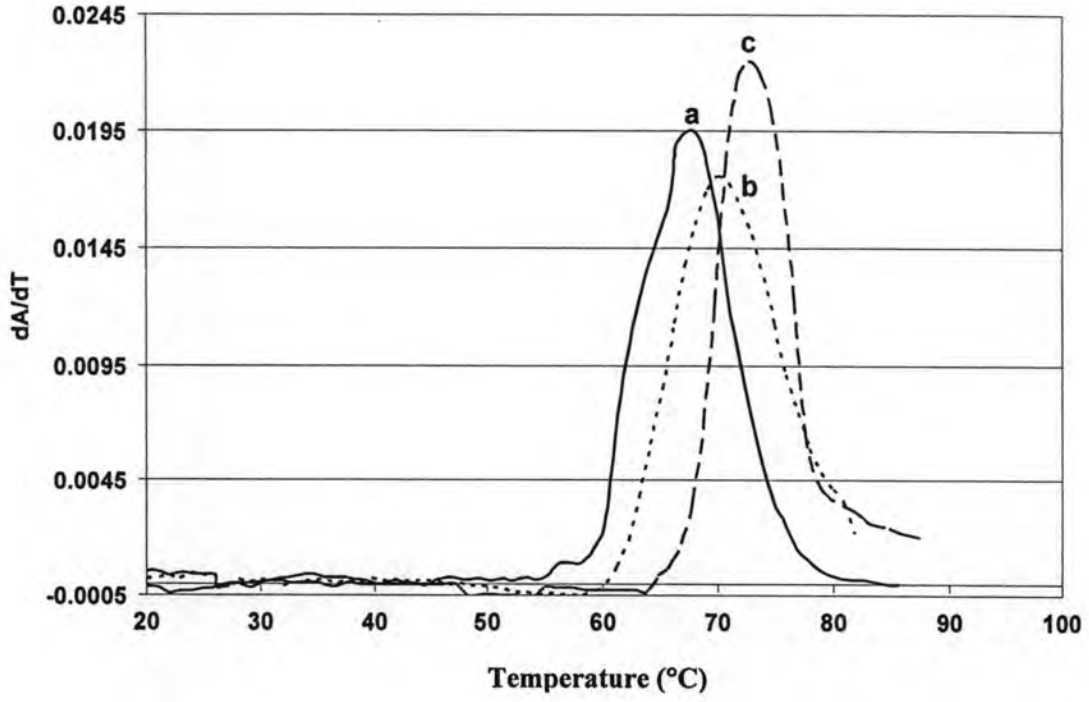

Fig. 12 Changes in absorbance (dA) with respect to increasing temperature (dT) at 260 nm for (a) ct-DNA, (b) ct-DNA with **2** and (c) ct-DNA with **1**.

3.3.1.3 CD spectroscopy

CD experiments were performed to study DNA binding properties of the compounds, which do not exhibit any optical activity in the absence of DNA. CD spectra were measured at various ratios of the compounds to DNA. In order to acquire the CD spectra of the **1**-DNA and **2**-DNA complexes presented in Fig. 13 and 14, measured amounts of the **1** and **2** solution were added to the ct-DNA solution at 25 °C. Since **1** is planar and chiral chromophore so it shows both the CD spectra of **1** and that of **1** bound with DNA. Whereas **2** are planar and achiral chromophore, it shows only the CD spectra of **2** bound with DNA. These may concern the molecules either bound at the chiral deoxyribose moieties on DNA or intercalated into DNA base pairs. Each binding mode involves particular surroundings and interactions for the molecules, so that the arising CD signals may display varied positions, signs and shapes.

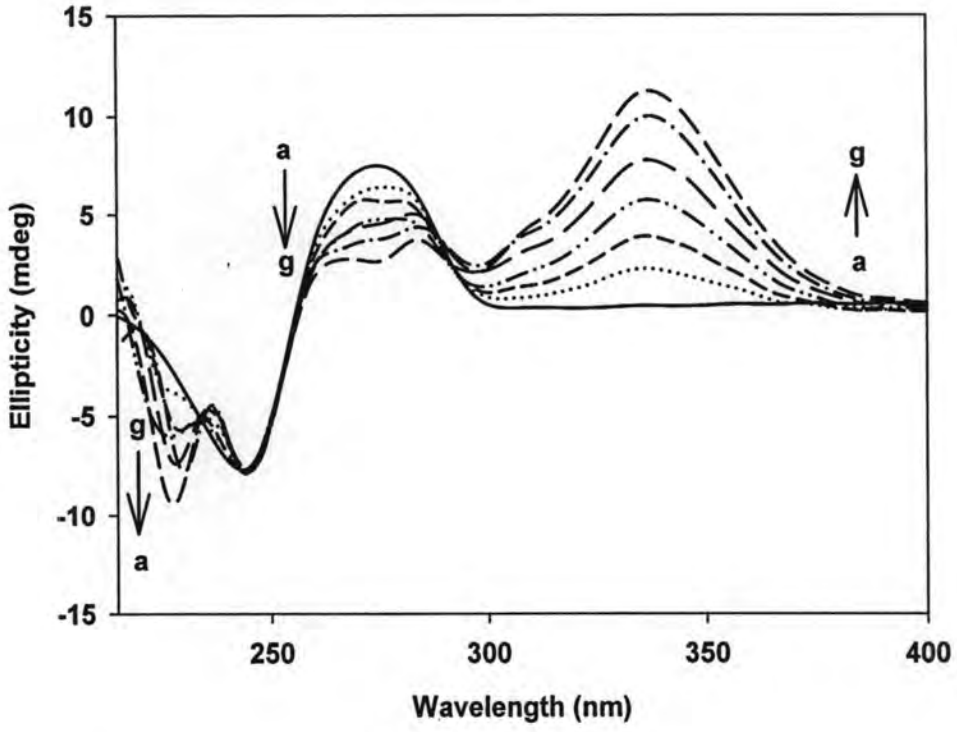

Fig. 13 Circular dichroism spectra of ct-DNA (0.12 mM) with increasing concentrations of **1** in 10 mM phosphate buffer (pH 7.0). Curves a to g denote ct-DNA treated with **1** ($x10^{-5}$ M) 0, 0.25, 0.5, 1.5, 2, 3, 4, 5, respectively.

Circular dichroism spectra provided direct evidence of the interaction of compounds with the asymmetric environment of the DNA helix. CD spectra of **1** and **2** with ct-DNA were recorded in the 200-400 nm regions.

As displayed in Fig. 13, the well-known CD spectrum of DNA is a conservative pattern with a positive band at approximately 276 nm and negative band at approximately 244 nm. The major effect of **1** on the CD spectrum of the DNA is to alter both the amplitudes and positions of the peaks of the positive and negative bands. Increasing the amount of **1** not only resulted in an increase in the negative band at 228 nm and a decrease in the positive bands at 276 nm but also led to an evident red shift of positive band (ca. 9 nm). Since **1** has chiral chromophore so it shows both the CD spectra of **1** and that of **1** bound with DNA. When adding the amount of **1** into DNA, the CD spectra were increased and little shifted from 336 to

337 nm. These spectra change suggests that a structural and/or conformational change has occurred when **1** bound DNA.

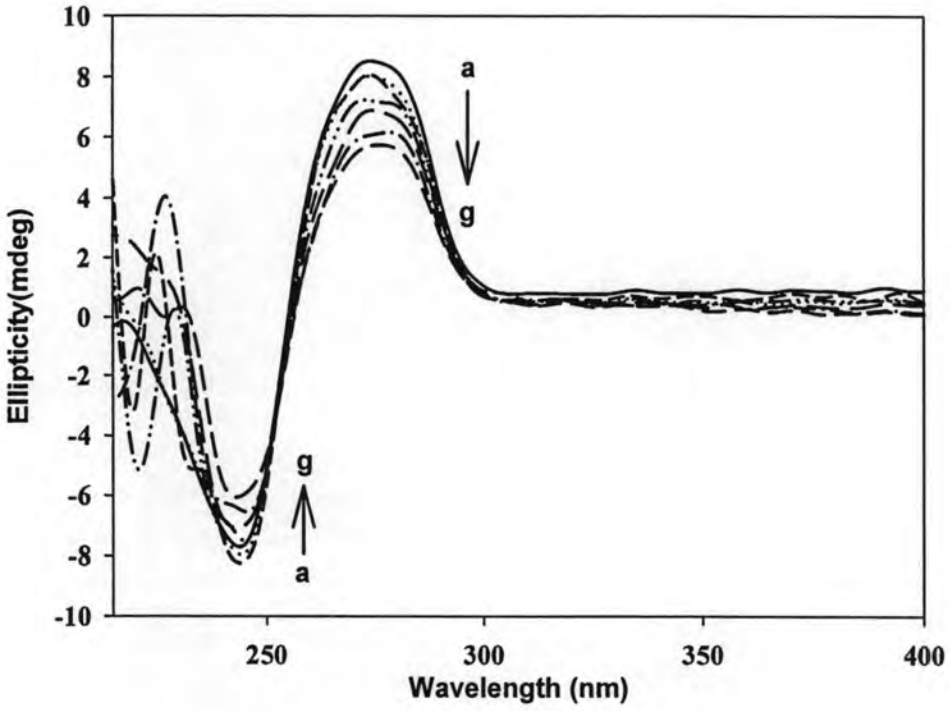

Fig. 14 Circular dichroism spectra of ct-DNA (0.12 mM) with increasing concentrations of **2** in 10 mM phosphate buffer (pH 7.0). Curves a to g denote ct-DNA treated with **2** ($x10^{-5}$ M) 0, 0.25, 0.5, 1.5, 2, 3, 4, 5, respectively.

The CD spectra of **2** with DNA showed in Fig. 14. A maximum positive CD at 274 nm and negative CD at 244 nm are induced when **2** is bound to DNA. The induced CD signals are due to the **2**-bound complex. Since **2** is an achiral molecule, optical activity is generated in the asymmetric environment of the DNA double helix. Increasing the amount of **2** not only resulted in an increase in the negative band at 227 nm and a decrease in the positive bands at 274 nm but also led to an evident red shift of positive band (ca. 2 nm). These spectra change suggests that a structural and/or conformational change has occurred when **2** bound DNA.

3.3.1.4 NMR studies

1D NMR studies of 1

The binding of **1** and **2** with d(CGTACG)$_2$ were studied by using ^{1}H-NMR spectroscopy. The changed chemical shift between the free and the bound forms are associated with the interaction between **1** and **2** with the base of DNA. To determine the feasibility of NMR studies on those compounds bound to DNA, **1** and **2** were titrated with d(CGTACG)$_2$ at different ratios.

1D spectra of 1 and d(CGTACG)$_2$

One dimensional ^{1}H-NMR spectra of **1**, the DNA duplex alone, and the complexes in the presence of 0.5, 1.0, 2.0 and 3.0 equivalents of **1** are shown in Fig. 15.

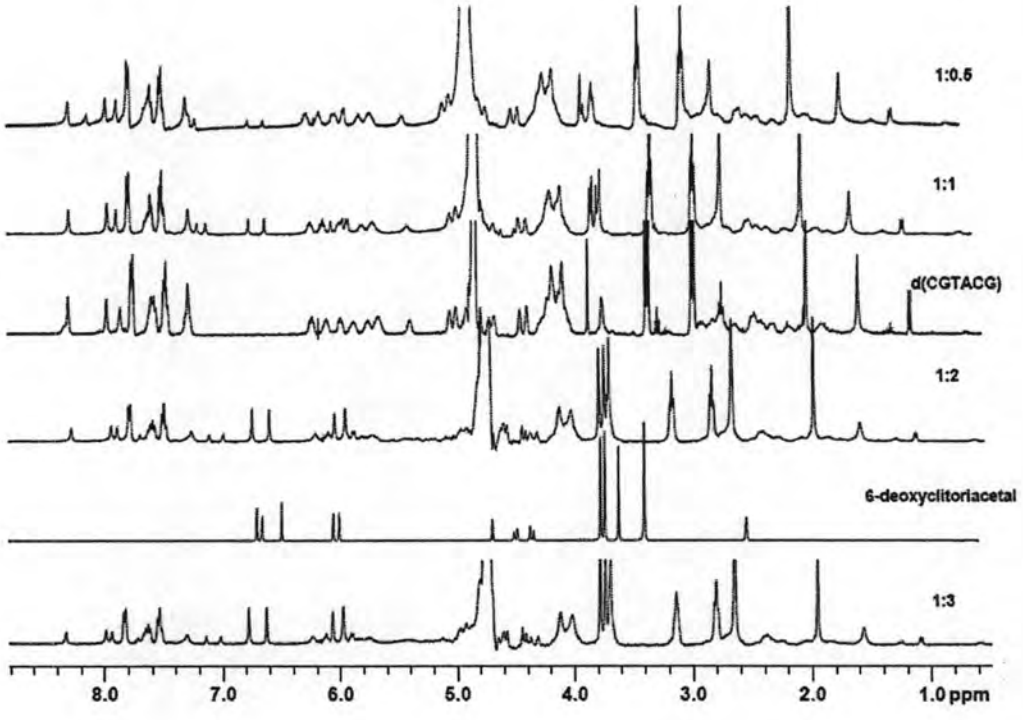

Fig. 15 One-dimensional ^{1}H-NMR titration of the free DNA, 1:0.5, 1:1, 1:2 and 1:3 of d(CGTACG)$_2$: 6-deoxyclitoriacetal complexes and free 6-deoxyclitoriacetal in the range of 2.0 to 8.0 ppm. The spectra were recorded at 300 K.

The spectra showed that some proton positions were shifted from their original positions in **1** and d(CGTACG)$_2$. The free **1** and free DNA have shape resonances. When the ratio of d(CGTACG)$_2$ to **1** are 1:0.5 and 1:1 respectively, the spectra show complex patterns. The complex was titrated until the ratio of 1:3. When the ratio reaches 1:2, the spectra become considerably simplified and similar to that of 1:3, showing that stable and symmetric 1:2 complexes are formed. Thus, the titration experiments indicated that full assignments of **1** with DNA at 1:2 ratios would be possible.

The interactions between **1** and d(CGTACG)$_2$ were investigated and followed the changed chemical shift of d(CGTACG)$_2$ when increasing the mole ratio of **1**. The chemical shift of **1** before and after binding with d(CGTACG)$_2$ were given in Table 4. The spectra showed that the position of hydroxyl (-OH), methoxy (-OMe) and aromatic protons of **1** were significantly changed from their original positions as follows:

(i) The –OH groups at C-11 and C12a (11.96 and 6.68 ppm) of **1** were absent after binding with d(CGTACG)$_2$, indicating that both –OH groups participated hydrogen bonding with DNA.

(ii) The –OMe groups were substantially identified three singlet patterns after binding with protons of d(CGTACG)$_2$ and exhibited the stable form at 1:2 ratios. All –OMe groups were shifted to downfield from 3.58 (a, 2-OMe), 3.70 (b, 9-OMe) and 3.73 (c, 3-OMe) ppm to 3.70 (a), 3.74 (b) and 3.78 (c) ppm, respectively. The 2-OMe and 3-OMe groups of ring A were correlated with the aromatic protons at H1 and H4 in the same ring, respectively. The largest changed position ($\Delta\delta$ = 0.12 ppm) was found at 2-OMe of ring A (Fig. 16). The results are corresponding with 2D-COSY experiments (Fig. 17).

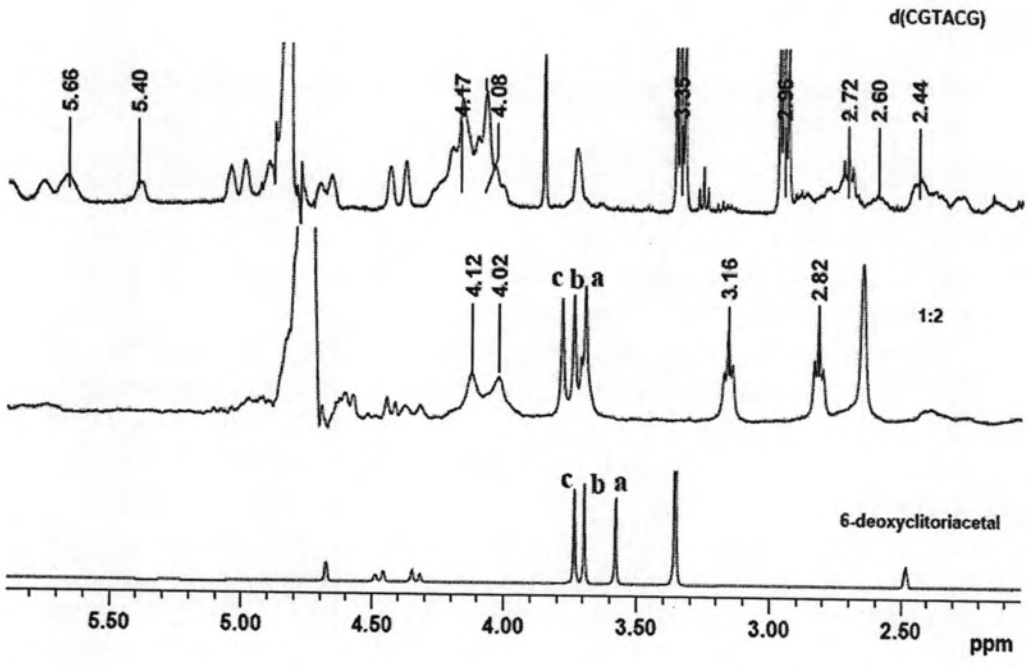

Fig 16 Expanded one-dimensional ^{1}H-NMR titration in the range of 2-6 ppm of **1** with DNA

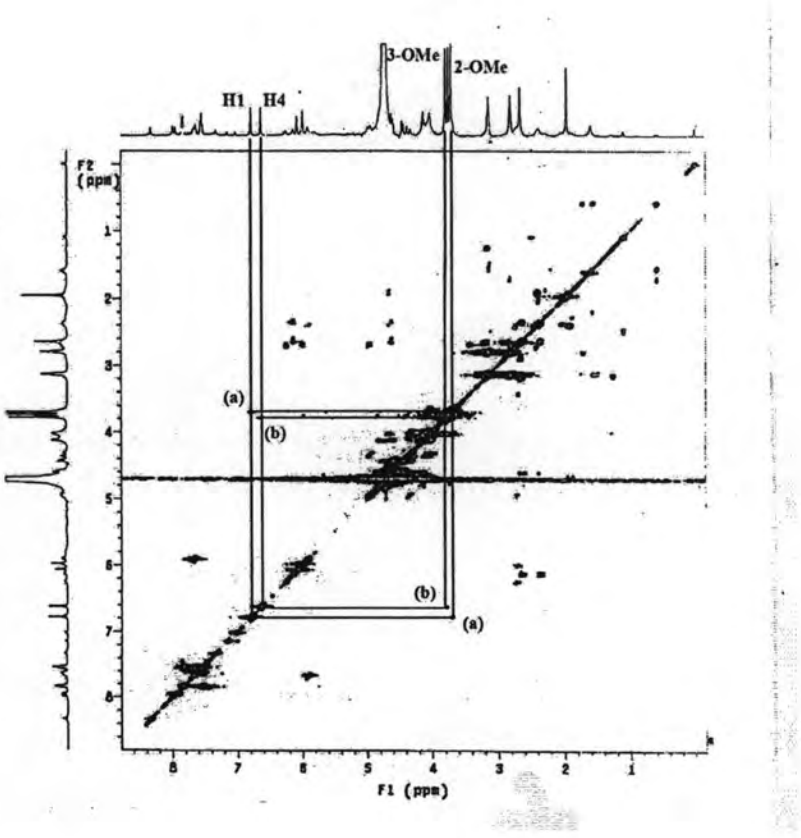

Fig 17 2D COSY spectra of complexation of **1** with d(CGTACG)$_2$ in the range of 1-8 ppm which provided information in the assignments of resonances. The sequential assignment pathway is indicated.

(iii) The aromatic protons of ring A at 6.51 (H1) and 6.73 (H4) ppm were shifted to downfield at 6.03 and 6.78 ppm and presented the strong signals when increasing the mole ratio of **1**. Whereas the protons of ring D at 6.01 (H8) and 6.06 (H10) ppm were clarified to singlet patterns and changed the line width of the original doublet pattern from 5 Hz to 2 Hz (Fig. 18). The changed chemical shift at aromatic protons was found both planar A and D, indicating that these planar planes involved in the binding with DNA. However, the downfield protons at H1 and H4 ($\Delta\delta$ = 0.05 and 0.12 ppm, respectively) revealed that the plane A was the important part in inserting into the adjacent base pairs of DNA in an intercalative like binding mode.

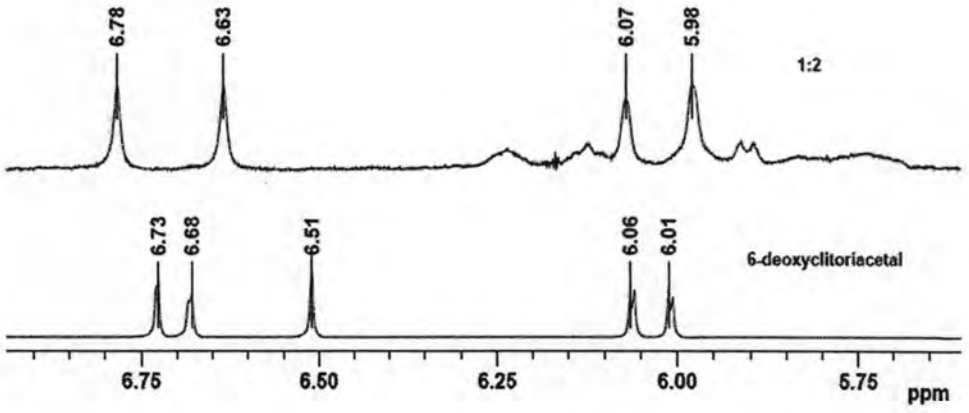

Fig 18 Expanded one-dimensional ^{1}H-NMR titration in the range of 5.75-6.75 ppm of **1** with DNA

Both the shifted of –OMe groups and aromatic protons identified that the planar ring A are associated with the intercalation into the adjacent base pairs of DNA. The most changed positions of –OMe protons and aromatic protons presented in planar ring A, showing that this planar may insert and tightly bind through the intermolecular interactions with $d(CGTACG)_2$.

The changed proton positions of $d(CGTACG)_2$ were found as well as that of **1** upon titration of **1**. Some proton positions of DNA were showed substantially either weak signal till absent or strong signal. However, the NMR spectra of $d(CGTACG)_2$ exhibited the broadening signal when binding with **1**. These may be involved the insertion of **1** into the adjacent base pairs. The changed spectra of $d(CGTACG)_2$ were investigated as follows:

(i) The amine proton region of cytosine and guanine was shown for different concentrations of **1** (Fig. 16). It is seen that the resonance of protons at 2.44 (C1), 2.60 (G6) and 2.72 (G2) ppm were substantially weak until absent whereas the protons at 4.08 (C1) and 4.17 (C5) ppm were broadened and upfielded shift to 4.02 and 4.12 ppm upon titration of **1**.

(ii) The proton positions at 5.40 (C5), 5.66 (C5) ppm were absent (Fig. 16). Furthermore, the substantial broadening protons at 7.31 (C5) ppm displayed at high concentrations of **1** (Fig. 19).

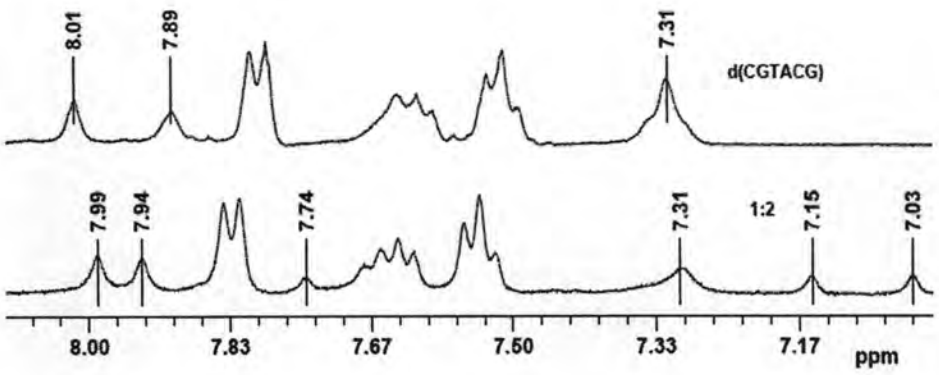

Fig. 19 Expanded one-dimensional ^{1}H-NMR titration in the range of 7-8 ppm of **1** with DNA

(iii) Interestingly, addition of increasing amounts of **1** to d(CGTACG)$_2$ resulted in the appearance of new proton position at 8.18 ppm in 1:0.5 ratio (Fig. 15). This peak was upfielded and exhibited at 7.74 ppm in ratio 1:2. Moreover, the other new peaks were displayed at 7.03 and 7.15 ppm (Fig. 19). The observed proton at 8.18 ppm (ratio 1:0.5) and then substantial constant at 7.74 ppm (ratio 1:2) may be concerned to the movement of –OH group at C11 in order to form the stable complex at 1:2 with DNA via the intermolecular interaction such as hydrogen bonding formation. Whereas, the presented new protons at 7.03 and 7.15 ppm may occur from the shielded protons of d(CGTACG)$_2$ from proton peak at 7.31 ppm. When the planar molecule of **1** insert into the base pairs at 7.31 ppm, the shielded aromatic protons were observed.

The 1D spectra titrations of d(CGTACG)$_2$ with **1** were observed and found that the changed proton positions of d(CGTACG)$_2$, **1** and the new obtained proton signals (Table 4) may be resulted from the intercalation and the binding of **1** with d(CGTACG)$_2$. Furthermore, the observed changing chemical shift of d(CGTACG)$_2$ were most prominent for the CpG base pairs and less obvious for ApT base pairs. These revealed that **1** may be intercalated the planar molecule into the base C and G.

The titration of d(CGTACG)$_2$ with **1** were significantly presented the shifted proton positions both **1** and d(CGTACG)$_2$. It can be concluded that **1** can bind with d(CGTACG)$_2$ by using the planar molecule of ring A insert into the space of adjacent base pairs of cytosine and guanine. The results were corresponding with the changed

chemical shift of both methoxy and aromatic protons at ring A of **1** and the protons of cytosine and guanine in d(CGTACG)$_2$.

Table 4 ^{1}H-NMR Chemical shifts (ppm) of d(CGTACG)$_2$, and 6-deoxyclitoriacetal (**1**) at 300 K [38]

Nonexchangeable proton chemical shifts of free and bound d(CGTACG)$_2$									
	H8/6	H5, H2, Me	H1'	H2'	H2''	H3'	H4'	H5'	H5''
C1 f-DNA	7.78	5.98	5.88	2.00	2.44	4.78	4.08		
b-DNA	7.82		5.90	1.95		4.65	4.02		
Δ	-0.04		-0.02	0.05		0.13	0.06		
G2 f-DNA	8.01		5.99	2.72	2.78	4.88	4.38		
b-DNA	7.99					4.86	4.34		
Δ	0.01					0.02	0.04		
T3 f-DNA	7.50	1.55	5.75	2.12	2.45	4.91	4.21		
b-DNA	7.54	1.55	5.76		2.43	4.87	4.18		
Δ	-0.04	0.00	-0.01		0.02	0.04	0.03		
A4 f-DNA	8.34	7.61	6.24	2.73	2.87	5.05	4.44		
b-DNA	8.35	7.63	6.24	2.72		5.02	4.42		
Δ	-0.01	-0.02	0.00	0.01		0.03	0.02		
C5 f-DNA	7.32	5.40	5.66	1.86	2.27	4.84	4.17		
b-DNA	7.21					4.84	4.12		
Δ	0.11					0.00	0.05		
G6 f-DNA	7.89		6.14	2.60	2.37	4.67	4.17		
b-DNA	7.94		6.13			4.63	4.12		
Δ	-0.05		0.01			0.04	0.05		

Nonchangeable proton chemical shifts of free and bound 6-deoxyclitoriacetal (**1**)									
	2-OMe	3-OMe	9-OMe	1	4	8	10	11	12a
f-1	3.58	3.73	3.70	6.73	6.51	6.01	6.06	11.96	6.68
b-1	3.70	3.78	3.74	6.78	6.63	5.98	6.07		
Δ	-0.12	-0.05	-0.04	0.05	-0.12	0.03	-0.01		

2D-NMR studies of 1 and d(CGTACG)$_2$

To clarify the bound position of **1** with d(CGTACG)$_2$, all the resonances of the stable complex **1** at 1:2 ratio observed from 2D NMR have been assigned and its chemical shifts are tabulated in Table 4. For the changed conformation of **1**, All methoxy groups were shifted to downfield. The COSY experiments of complexes can be confirmed that the 2-OMe group (ring A) at 3.58 ppm were shifted to 3.70 ppm and correlated with the aromatic protons at H1 in the same ring (Fig. 17a) while the 3-OMe group (ring A) at 3.73 ppm was shifted to 3.78 ppm and correlated with the aromatic protons at H4 (Fig. 17b). Hence, the residue –OMe group belongs to 9-OMe and it shifts to downfield from 3.70 to 3.74 ppm. In the case of d(CGTACG)$_2$, the largest changes in chemical shifts between the free and the bound forms of d(CGTACG)$_2$ are associated with the C1H4' ($\Delta\delta$ = +0.06 ppm) and C5H4' ($\Delta\delta$ = +0.05 ppm). These data supported the idea that the planar molecule of **1** is sandwiched between the two cytosines so that the ring current effects mutually affected their chemical shifts. The inspection of the 2D NOESY spectra (Fig. 20) revealed that the H10 and H8 protons at ring D are correlated to 2-OMe and 3-OMe (ring A) (Fig. 20a). In addition, the H8 of **1** are closed to C5H6 (Fig. 20b) as well as the closed protons of H10 of **1** with G6H8 and G6H2" (Fig. 20c). These suggested that ring D and ring A of **1** are sandwiched between C1 and C5. The assignment of the resonance of the complex was established by starting with the aromatic – H1' fingerprint region using the sequential assignment strategy and compared the spectra with the 2D NOESY of d(CGTACG)$_2$ (Fig. 21). It is clear that the peak of C5H5 was absent after binding with **1** (Fig. 21a), while the intensities between the C5H6-G6H8 crosspeaks (Fig. 21b, 20d) are significantly weaker than those of the other internucleotide crosspeaks. The aromatic proton at H10 of **1** overlapped the aromatic protons of G2H1'. It resulted the absence crosspeaks at C5H6, C5H4', G2H8, G2H4' and G6H4'.

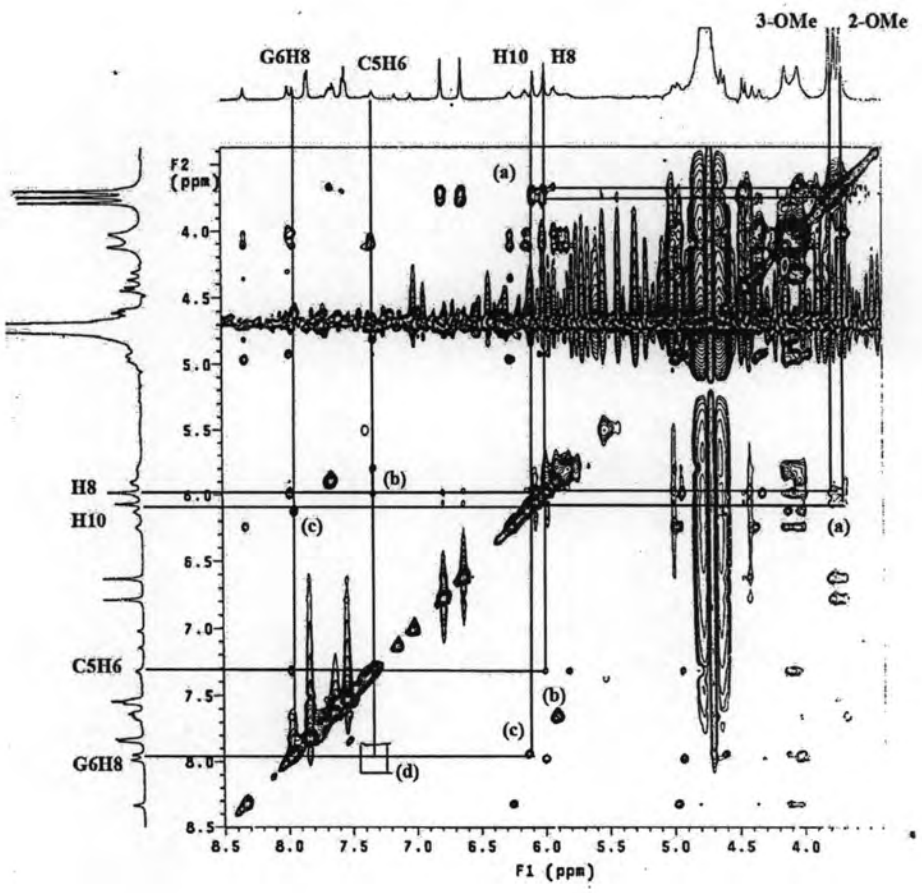

Fig. 20 Expanded aromatic to H1' region (5-8.5 ppm) of 2D NOESY spectra of complexation of **1** with d(CGTACG)$_2$ which provided information in the assignments of resonances. The sequential assignment pathway is indicated.

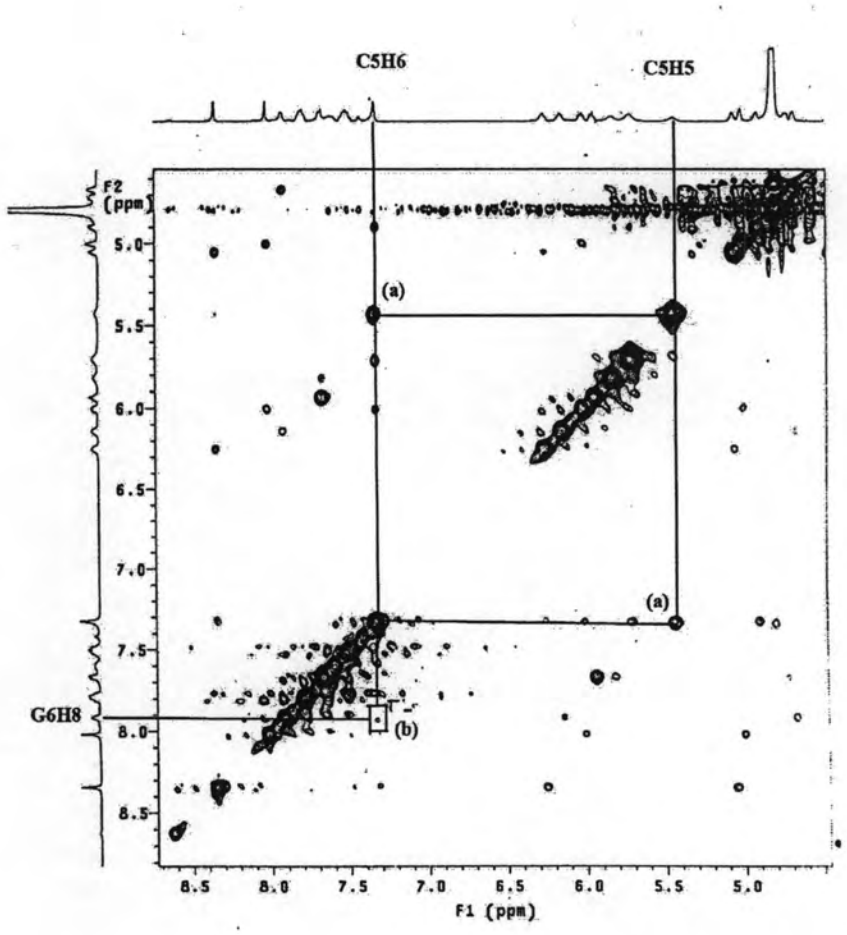

Fig. 21 Expanded aromatic to H1' region (5-8.5 ppm) of 2D NOESY spectra of d(CGTACG)$_2$ which provided information in the assignments of resonances. The sequential assignment pathway is indicated.

1D spectra of 2 and d(CGTACG)$_2$

One dimensional ^{1}H-NMR spectra of **2**, the DNA duplex alone, and the complexes in the presence of 0.5, 1.0, 2.0 and 3.0 equivalents of **2** are shown in Fig. 22.

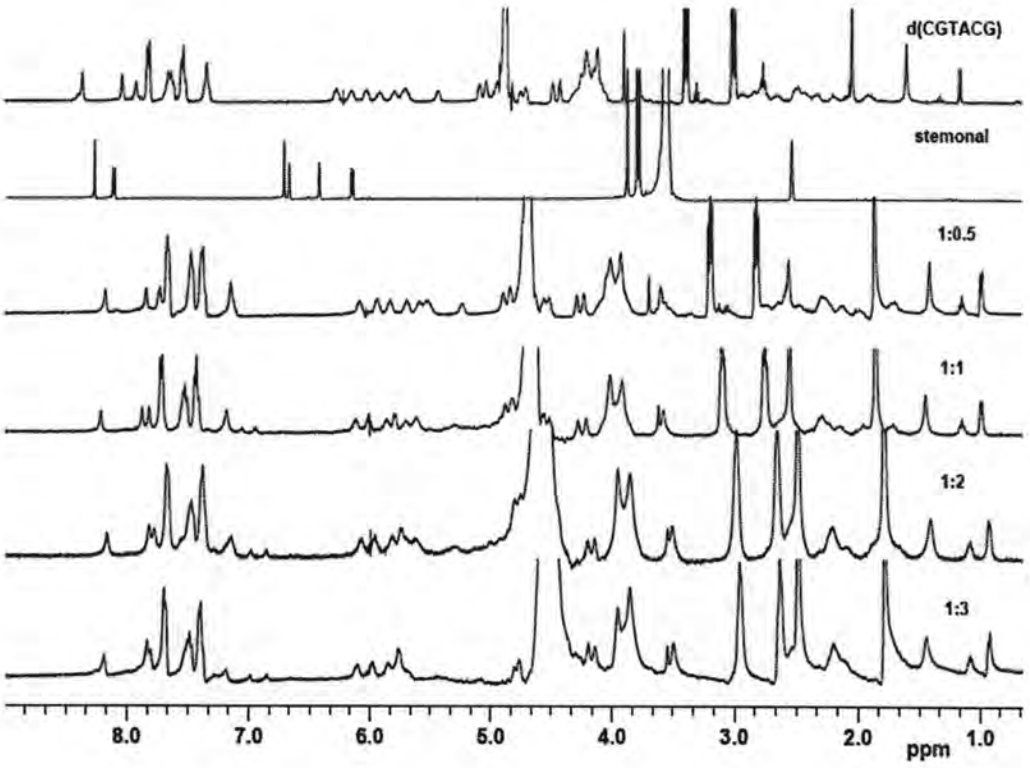

Fig. 22 One-dimensional ^{1}H-NMR titration of the free DNA, 1:0.5, 1:1, 1:2 and 1:3 of d(CGTACG)$_2$: stemonal complexes and free stemonal in the range of 2.0 to 8.0 ppm. The hydroxyl group at C11 (12.77 ppm) were omitted for clarify. The spectra were recorded at 300 K.

The spectra showed that some proton positions were shifted from their original positions in **2** and d(CGTACG)$_2$. The free **2** and free DNA have shape resonances. When the ratio of d(CGTACG)$_2$ to **2** are 1:0.5 and 1:1 respectively, the spectra show complex patterns. The complex was titrated until the ratio of 1:3. When the ratio reaches 1:2, the spectra become considerably simplified and similar to that of 1:3, showing that stable and symmetric 1:2 complexes are formed. Thus, the titration experiments indicated that full assignments of **2** with DNA at 1:2 ratios would be possible.

The same sequence DNA was titrated and studied the binding ability with **2**. The interactions between **2** and d(CGTACG)$_2$ were investigated and followed the changed chemical shift of d(CGTACG)$_2$ when increasing the mole ratio of **2** (Fig. 22). The chemical shift of d(CGTACG)$_2$ before and after binding with **2** were given in Table 5. The OH group at C-11 (12.77 ppm) of **2** was absent when binding with d(CGTACG)$_2$. This is similar to that of **1**. In the case of DNA, the spectra of

$d(CGTACG)_2$ were substantially changed when increasing the mole ratio of **2** as follows:

(i) The amine proton region of cytosine and guanine was shown for different concentration of **2** (Fig. 23). It is seen that the resonance of protons were shifted to upfield from 2.27 (C5), 2.96 and 3.35 ppm to 2.21, 2.65 and 2.99 ppm, respectively. This is similar to the upfielded protons at 2.00 to 1.79 ppm of C1.

(ii) The changed chemical shift of cytosine and guanine from 4.08 (C1), 4.17 (C5) and 4.38 (G2) ppm to 3.85, 3.95 and 4.15 ppm, respectively as well as the upfielded adenine proton from 4.44 ppm of original DNA to 4.20 ppm (Fig. 23).

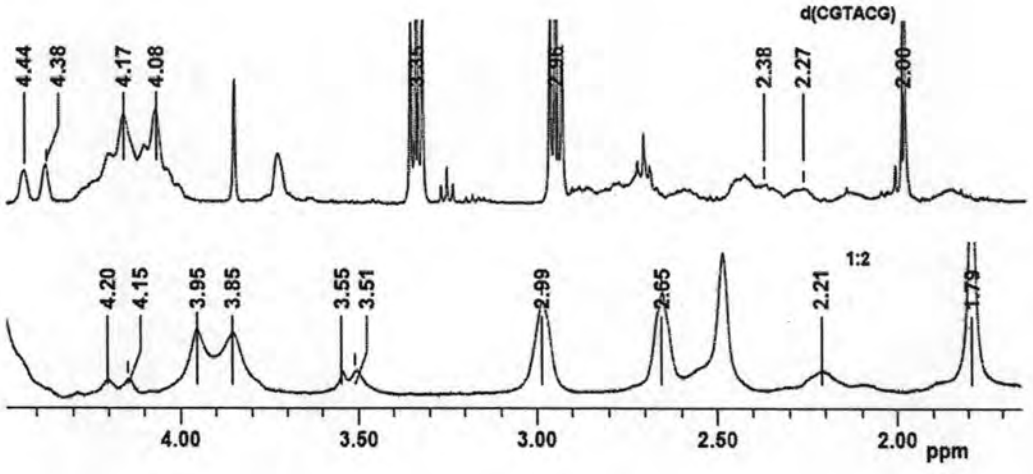

Fig. 23 Expanded one-dimensional ^{1}H-NMR titration in the range of 2-4 ppm of **2** with DNA

(iii) The protons between 5.4 to 6.3 ppm of $d(CGTACG)_2$ (Fig. 24) were shifted to upfield from 5.68 (C5), 6.00 (G2), 6.12 (G6), 6.24 (A4) ppm to 5.62, 5.81, 5.96, 6.08 ppm with the influence of mixed solvents and intercalation of **2**. The proton signal at 5.4 ppm (C5) was substantial broadened and shifted to upfield at 5.28 ppm. Furthermore, the double protons at 5.74 ppm ($J = 4$ Hz) were presented because of the coupling between the protons at 5.76 (T3) and 5.89 (C1) ppm and the effect of mixed solvent.

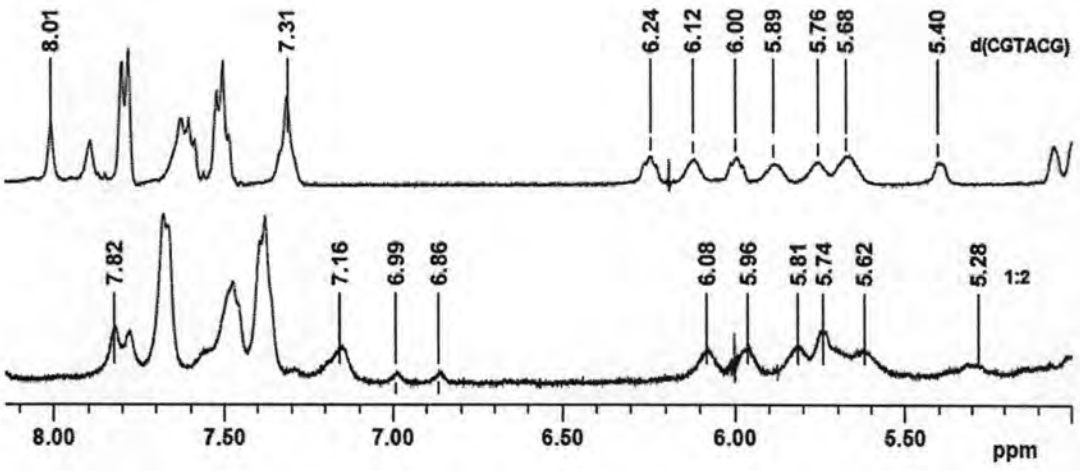

Fig. 24 Expanded one-dimensional ^{1}H-NMR titration in the range of 6-8 ppm of **2** with DNA

(iv) The aromatic protons region (Fig. 24) were shifted to upfield, especially the proton position of guanine at 8.01 (G2) ppm was shifted to 7.82 ppm. This is similar to the proton at 7.31 (C5) ppm was broadened and shifted to upfield to 7.16 ppm. Interestingly, the new protons at 6.86 and 6.99 ppm were observed. The new protons may result from the insertion of **2** into d(CGTACG)$_2$. This attributed to decrease the shielded aromatic protons that closed place with the proton at 7.31 ppm. Also, the new peaks were separated. These are the same characteristic protons as found new protons in complexation of **1** with d(CGTACG)$_2$.

Although, the ^{1}H-NMR spectra of **2** was showed only the absent of –OH proton. From the 1D NMR titration showed that **2** may involve in the changing of ^{1}H-NMR of d(CGTACG)$_2$ and exhibited the unique complexation pattern which was difference from the complexation of **1**. These may associate with the difference stable binding abilities and the conformations in compounds **1** and **2**.

The interaction between **1** and **2** was studied from the following 1D NMR titrations between **1** and **2** with d(CGTACG)$_2$. The results showed the slow exchange of d(CGTACG)$_2$. It can be concluded that both **1** and **2** intercalate into the adjacent base pairs. These are considered from the changed ^{1}H-NMR spectrum of

$d(CGTACG)_2$ upon titration with compounds. However, the shifted ^{1}H-NMR of $d(CGTACG)_2$ from those compounds are different pattern. The binding of **1** with $d(CGTACG)_2$ exhibited the slow changed conformation of **1** till the stable mixing ratio at 1:2 as well as the broadening of $d(CGTACG)_2$ spectra. The most changed chemical shift were found and correlated with the chemical shift of C1pG2 and C5pG6 site, indicating that **1** prefer to insert its planar molecule into between CpG base pairs. In the case of the binding of **2** with DNA, it was only followed the slow changed chemical shift of $d(CGTACG)_2$ till the formation of stable complexation at the same mixing ratio with **1**. It can be proposed that the molecule of **2** really inserted into the $d(CGTACG)_2$ or intercalated in the outside of $d(CGTACG)_2$. However, from 1D NMR titration, the new peaks at 6.86 and 6.99 ppm were observed, and found the changed chemical shift at C1pG2 and C5pG6, indicating that the planar molecule of **2** may be involved in the insertion into the CpG base pairs as well as that of **1**.

Table 5 ^{1}H-NMR Chemical shifts (ppm) of d(CGTACG)$_2$, and stemonal (**2**) at 300 K [38]

Nonexchange Proton Chemical Shifts of Free and Bound d(CGTACG)$_2$									
	H8/6	H5, H2, Me	H1'	H2'	H2''	H3'	H4'	H5'	H5''
C1 f-DNA	7.78	5.98	5.89	1.99	2.44	4.78	4.08		
b-DNA	7.67	5.85	5.74	1.79	2.20	4.36	3.85		
Δ	0.11	0.13	0.15	0.20	0.24	0.42	0.23		
G2 f-DNA	8.01		6.00	2.70	2.78	4.88	4.38		
b-DNA	7.82		5.81			4.68	4.15		
Δ	0.19		0.19	0.16		0.20	0.23		
T3 f-DNA	7.50	1.55	5.76	2.15	2.45	4.91	4.21		
b-DNA	7.39	1.44	5.74		2.20	4.67	3.95		
Δ	0.11	0.11	0.02		0.25	0.24	0.16		
A4 f-DNA	8.34	7.61	6.24	2.73	2.87	5.05	4.44		
b-DNA	8.18	7.48	6.08	2.54		4.80	4.20		
Δ	0.16	0.13	0.15	0.19		0.25	0.24		
C5 f-DNA	7.31	5.40	5.68	1.86	2.27	4.84	4.17		
b-DNA	7.16	5.28	5.62		2.21	4.52	3.95		
Δ	0.15	0.12	0.06		0.06	0.32	0.22		
G6 f-DNA	7.93		6.12	2.61	2.38	4.67	4.17		
b-DNA	7.80		5.96			4.25	3.95		
Δ	0.13		0.16			0.42	0.22		

2D-NMR studies of 2 and d(CGTACG)$_2$

All resonance of bound position of **2** with d(CGTACG)$_2$ at 1:2 ratio was observed from 2D NMR (Fig. 8) and assigned its chemical shifts (Table 5). The largest changes in chemical shifts between the free and the bound forms are associated with the C1H3' ($\Delta\delta$ = +0.42 ppm) and C5H4' ($\Delta\delta$ = +0.32 ppm). These data supported the idea that the planar molecule of **2** can sandwich between the two cytosines so that the ring current effects mutually affected their chemical shifts as

well as **1**. The assignment of the resonance of the complex was established by starting with the aromatic – H1' fingerprint region using the sequential assignment strategy. Interestingly, the new crosspeak between the aromatic protons at 6-7 ppm with the amine proton at 2-3 ppm of cytosine and guanine (Fig. 25) were found. This is similar to the found crosspeak in the range of the aromatic – H1' because the correlation between aromatic protons at 6-7 ppm with 7-8 ppm of cytosine and guanine (Fig. 25b). In addition, the new crosspeak between G6H8 with C5H6 was presented in the complexation of **2** (Fig. 25c). Whereas, the intensities at C5H6 correlated with the other protons in the same cytosine base were absent. For example, the absent resonance protons between C5H6 with C5H4', G6H4' (Fig. 8d) and C5H5 (Fig. 25e) were found. These new cross peaks may be resulted from the binding between **2** with $d(CGTACG)_2$. However, it can not form the stabilizing complex because the molecule of **2** having the OH group at C6, this may be the steric hindrance in the intercalation of **2** into $d(CGTACG)_2$. It resulted the binding of **2** with $d(CGTACG)_2$ occur only the aromatic part of **2** with the aromatic part of $d(CGTACG)_2$. Moreover, the shield between aromatic proton of $d(CGTACG)_2$ and the aromatic part of **2**, it may cause the disappearance of all protons of **2**. However, the found crosspeaks can be confirmed that some planar part of **2** can insert into the CpG base pair.

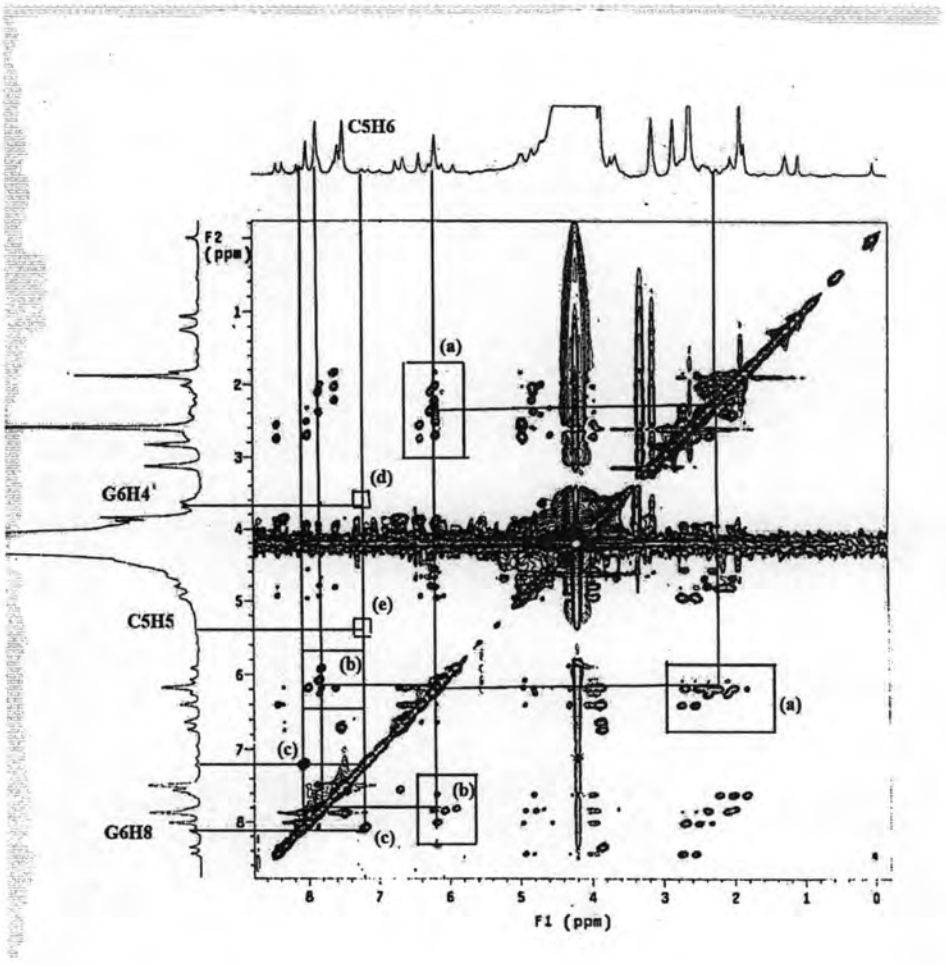

Fig. 25 2D NOESY spectra of complexation of **2** with d(CGTACG)$_2$ in the range of 0-8 ppm which provided information in the assignments of resonances. The sequential assignment pathway is indicated.

In comparison with the previously reported, it showed that the intercalative site of **1** and **2** bound d(CGTACG)$_2$ at CpG investigated from 1D and 2D NMR spectroscopy were the same site as Daunomycin, derivative of Doxorubicin HCl, bound with the same sequence DNA. Although, two middle DNA sequence of d(CGTACG)$_2$ have been switched to d(CGATCG)$_2$, Doxorubicin HCl and Daunomycin have been preserved the intercalative site at CpG. In Doxorubicin HCl - d(CGATCG)$_2$, the aglycon moiety intercalates in the DNA hexamers, between the G-C base pairs on either end of the duplex. These features were found in the complexes

of **1** and **2** as well at C1pG2 and C5pG6. However, the different structure between **1** and **2** may be involved the binding ability with DNA and effected to the NMR patterns of each complexation. These may associate with the only presence of bent shape at C6a-C12a in **1**. Although, **1** and **2** can intercalate into the CpG pairs, **1** showed the strong binding ability with DNA because of the feasibility of changed chemical shift and conformation both **1** and $d(CGTACG)_2$. The planar molecule of **1** insert into between CpG base pairs and form the stable complexation with $d(CGTACG)_2$ by using its bent shape to bind strongly as an anchor with $d(CGTACG)_2$ via the intermolecular interactions such as the hydrogen binding, whereas **2** has only planar molecule thus the loose binding with DNA and less stable complexation were formed.

All 1D and 2D NMR experiments, it revealed that the stable complex was established between **1** with $d(CGTACG)_2$ by considering from the following changed conformation both **1** and $d(CGTACG)_2$. Whereas, the molecule of **2** may insert and capable moving to the outsize due to less tight binding ability with $d(CGTACG)_2$. This can be concluded that the stable complex of **2** can not be formed like that of **1**. These NMR data were corresponding with the difference in the anticancer activities between **1** and **2**. The intercalating and strong binding of **1** with $d(CGTACG)_2$ may cause the distort and no longer have the normal B-DNA backbone conformation. The changed conformation of $d(CGTACG)_2$ effect to the abnormal replication and transcription process. These results attribute to present the good anticancer activities of **1** in various types of cancer. Although, the molecule of **2** can intercalate and insert its planar molecule into $d(CGTACG)_2$, it can not be formed the stabilized complex with $d(CGTACG)_2$. This made **2** having less activity than **1**.

The mixed solvent effect in NMR titration

For the NMR titration, **1** and **2** were dissolved in DMSO-d_6 and titrated in the $d(CGTACG)_2$ in D_2O solution. Therefore, the shift of overall protons may associated with the influence of used mixed solvent between DMSO-d_6 and D_2O. The experiments can be confirmed from the following the titrated $d(CGTACG)_2$ in D_2O with DMSO-d_6 to determine the changed pattern of $d(CGTACG)_2$. In Fig. 26, the $d(CGTACG)_2$ in D_2O were added with DMSO-d_6 in the same equivalent with the compounds **1** or **2**. The $d(CGTACG)_2$ - 1 to - 3 referred to increase the DMSO-d_6 at ratio 1:0.5, 1:1 and 1:2, respectively. These can be identified that the shifted protons

in both complexes occur from the influence of the mixed solvent or the insertion of **1** and **2** into the base pairs DNA. In particular, for complex of **2**, the changed conformation of **2** can not be followed whereas only changed chemical shift of $d(CGTACG)_2$ were observed. This study can be clarified that the changed chemical shift of $d(CGTACG)_2$ when binding with **2** caused from the insertion of the planar molecule of **2** into the CpG base pairs or the solvent effect. The results showed that the mix solvents effected to the appearance of double protons at 5.75 ($J = 4$ Hz). The other proton positions showed the little downfield shilft whereas the changed proton signals of $d(CGTACG)_2$ in those complexes were found in the upfield shift. Moreover, it can be concluded that the found new proton signals were not associated with the used mix solvents.

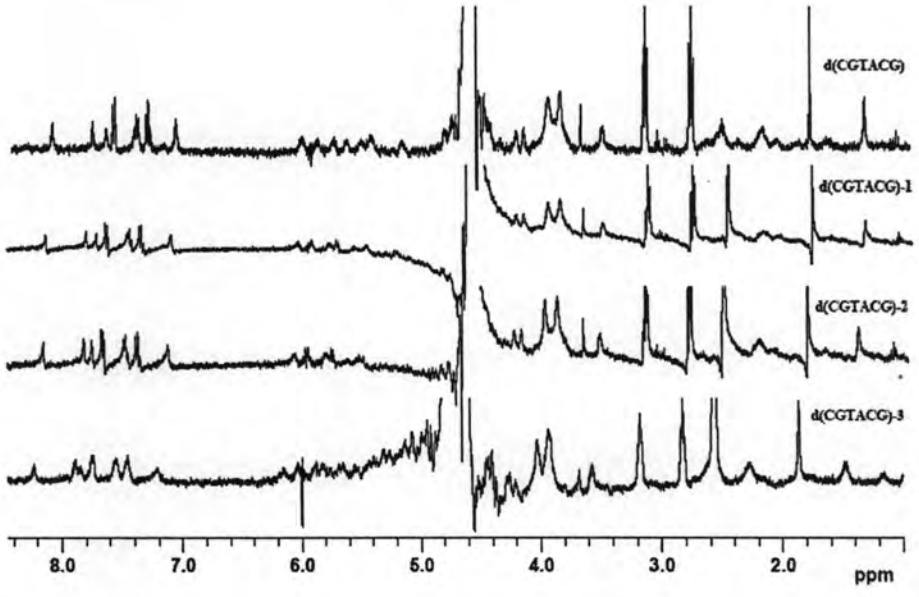

(a)

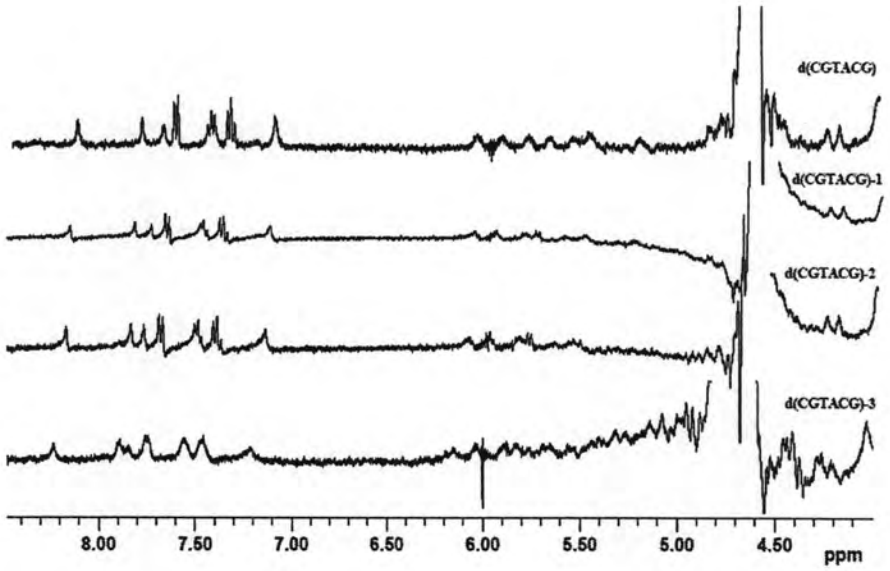
d(CGTACG)
d(CGTACG)-1
d(CGTACG)-2
d(CGTACG)-3
8.00
7.50
7.00
6.50
6.00
5.50
5.00
4.50
ppm

(b)

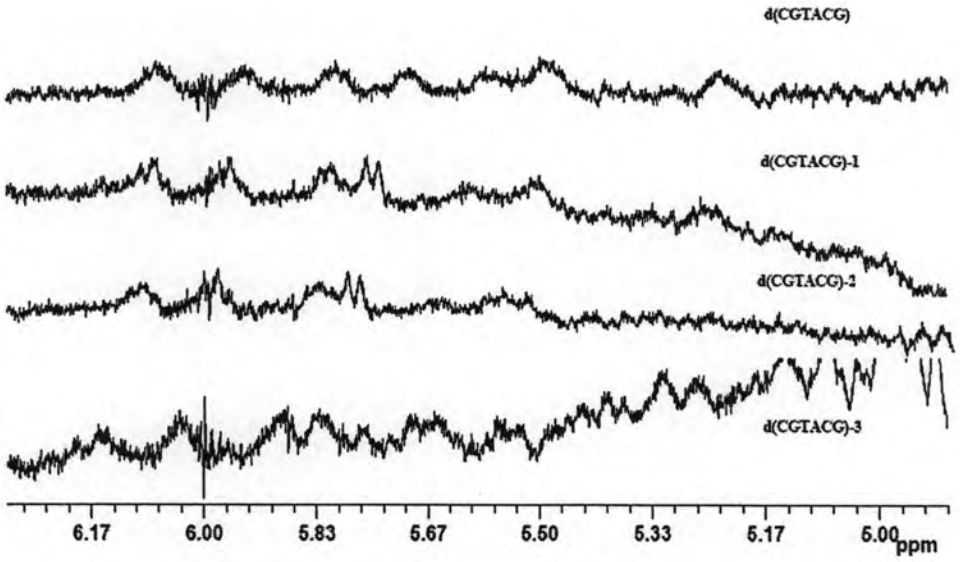
d(CGTACG)
d(CGTACG)-1
d(CGTACG)-2
d(CGTACG)-3
6.17
6.00
5.83
5.67
5.50
5.33
5.17
5.00
ppm

(c)

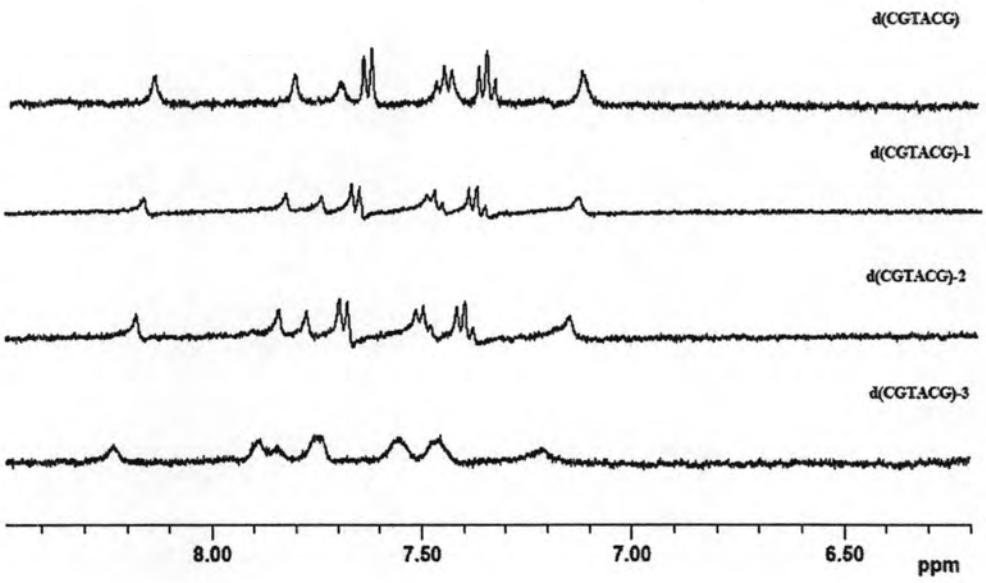

(d)

Fig 26 One-dimensional ^{1}H-NMR titration of the free DNA in D_2O with DMSO-d_6 The d(CGTACG)$_2$ - 1 to - 3 referred to increase the DMSO-d_6 at ratio 1:0.5, 1:1 and 1:2, respectively.

In addition to the intermolecular interaction study of **1** and **2** with DNA by using NMR spectroscopy, the binding ability of compounds with DNA can be determined from the compared melting temperature of DNA before and after binding with each compound.

3.4 Synthesis of 6-deoxyclitoriacetal analogues

6-Deoxyclitoriacetal is a model anticancer substance being used to study the structure-activity relationship. Both the planar structure and bent shape help to stabilize the intercalation between 6-deoxyclitoriacetal and DNA base pairs. It can be confirmed by the results of cytotoxicity against three cancer cell lines, KB (Human mouth carcinoma), MCF7 (Breast cancer) and NCL-H187 (Human small lung cancer) cell lines. It was found that 6-deoxyclitoriacetal showed the IC_{50} value of 0.08, 0.26 and 0.04 μg/ml when compared with the IC_{50} value of positive control, doxorubicin, with 0.33, 0.82 and 0.04 μg/ml in KB (Human mouth carcinoma), MCF7 (Breast cancer) and NCL-H187 (Human small lung cancer) cell lines, respectively.

As a knowledge of the intercalation mechanism of doxorubicin to inhibit the cytotoxic activity, this compound is composed of a planar aromatic moiety and a six-member daunosamine sugar moiety, forming a bent-shape molecule. The planar aromatic moiety can intercalate between two base pairs of DNA, while daunosamine sugar moitey can increase binding activity with base pairs of DNA at the intercalating sit by hydrogen bonding.. We propose that not only the planar aromatic molecule is the important factor in the intercalation process, but also the bent shape molecule can help to stabilize the drug-DNA complex via the intermolecular interaction such as hydrogen bonding, π-π interaction. Therefore, the derivatives of 6-deoxyclitoriacetal were synthesis to study the abovementioned factors, and then study the structure-relationship by testing for their cytotoxicities with various cell lines, furthermore, study the ability to inhibit the Topoisomerase II. The preferred functional groups are the flexible functional groups with strongly hydrogen bonding to the base pairs of DNA and help stabilization of the substance-DNA intercalation, for example, amino acid, aromatic carboxylic acid and the derivatives of pyrimidine base.

3.4.1 The 6-deoxyclitoriacetal – amino acid analogues

Amino acids play a central role both as building blocks of proteins and as intermediates in metabolism. Many potential anticancer substances are composed of amino acids as a part of molecules [52]. Therefore, in this work the structure of 6-deoxyclitoriacetal were modified with certain amino acids. In order to study the

effect of functional group of amino acid and the effect of the side chain-length of amino acid on the cytotoxicity, five amino acids were chosen to synthesize with 6-deoxyclitoriacetal, namely glycine, alanine, isoleucine, cystein and arginine. Compound **A** is the epoxide derivative of 6-deoxyclitoriacetal. Compounds **A1** to **A5** are the products of the epoxide ring-opening of 6-deoxyclitoriacetal with amino acids mentioned above. The reaction scheme was shown in Scheme 16. The details of the spectroscopy characterization including ^{1}H-NMR, ^{13}C-NMR and LC-ESI mass spectroscopy for all the compounds were given in Table 6 to 11

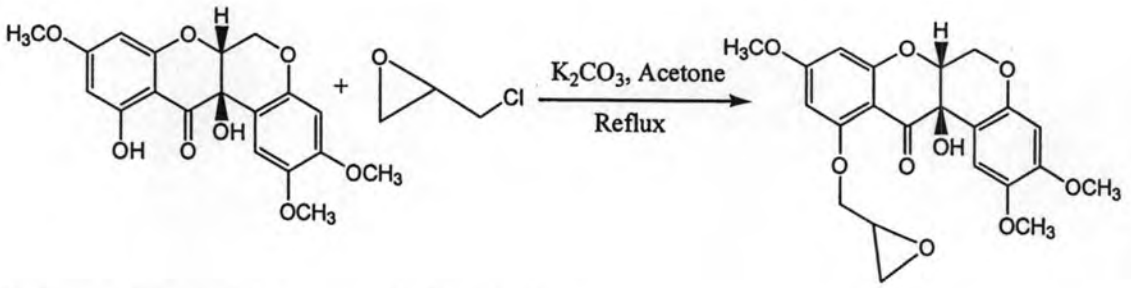

6-deoxyclitoriacetal epichlorohydrin **A**

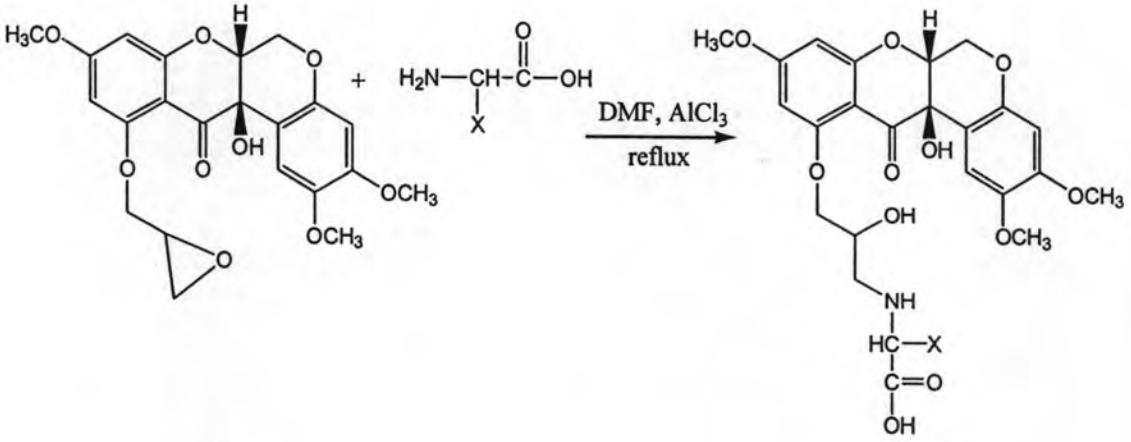

A **A1** to **A5**

A1, X = H; **A2**, X = CH_3; **A3**, X = CH_3, $(CH_3)CHCH_2CH_3$; **A4**, X = CH_2SH
A5, X = $(CH_2)_3NHC(NH)(NH_2)$

Scheme 16 Synthesis pathway for compounds **A, A1 to A5**

Table 6 Characterization the 6- deoxyclitoriacetal analogues (**A**)

Compound	Name	Structure	MW.	^{1}H NMR	^{13}C NMR
A	12a-Hydroxy-2,3,9-trimethyl-11-oxiranylmethoxy-6a,12a-dihydro-6*H*-chromeno[3,4-*b*]chromen-12-one	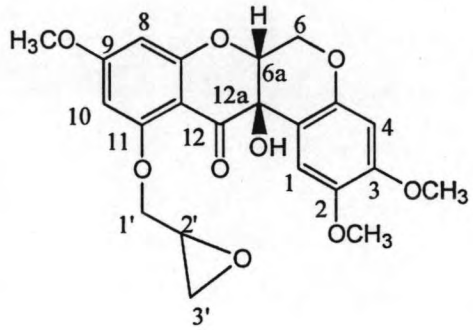	452.6 $[M+Na]^{+}$	3.67 (s, 3H, OMe-2), 3.68 (s, 3H, OMe-9), 3.73 (s, 3H, OMe-3), 4.38 (dd, *J* = 12.0, 2.0 Hz, 1H, H-6), 4.46 (d, *J* = 2.3 Hz, 1H, H-6a), 4.51 (dd, *J* = 12.0, 2.3 Hz, 1H, H-6), 5.96 (d, *J* = 1.8 Hz, 1H, H-8), 6.40 (d, *J* = 1.7 Hz, 1H, H-10), 6.44 (s, 1H, H-4), 6.46 (s, 1H, H-1), 2.96 (dd, *J* = 2.5, 5.0 Hz, 1H, C3′-Ha), 3.02 (dd, *J* = 2.5, 5.0 Hz, 1H, C3′-Hb), 3.32-3.35 (m, 1H, C-2′H), 3.95 (dd, *J* = 4.4, 11.3 Hz, 1H, C1′-Ha), 4.04 (dd, *J* = 4.7, 11.3 Hz, 1H, C1′-Hb)	55.6 (OMe-9), 55.8 (OMe-3), 56.4 (OMe-2), 63.8 (C-6), 67.1 (C-12a), 75.7 (C-6a), 94.0 (C-8), 94.5 (C-10), 101.0 (C-4), 102.2 (C-1a), 109.4 (C-1), 142.1 (C-2), 148.2 (C-4a), 151.0 (C-3), 161.4 (C-7a), 164.2 (C-11), 168.8 (C-9), 195.0 (C-12), 44.6 (C3′), 49.9 (C-2′), 75.7 (C-1′)

Table 7 Characterization the 6- deoxyclitoriacetal analogues (**A1**)

Compound	Name	Structure	MW.	^{1}H NMR	^{13}C NMR
A1	[2-Hydroxy-3-(12a-hydroxy-2,3,9-trimethoxy-12-oxo-6,6a,12,12a-tetrahydro-chromeno [3,4-*b*] chromen-11-yloxy)-propylamino]-acetic acid	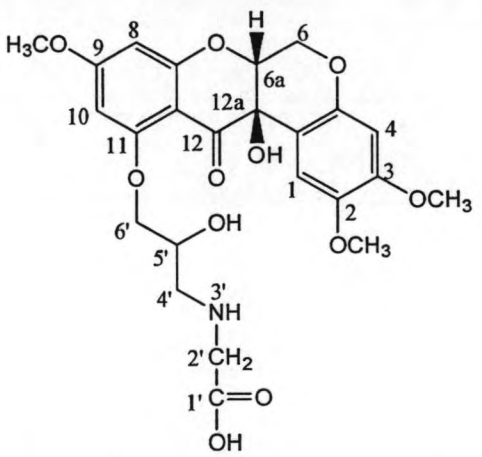	543.4 $[M+K]^{+}$	3.72 (s, 3H, OMe-2), 3.77 (s, 3H, OMe-9), 3.80 (s, 3H, OMe-3), 4.45 (dd, *J* = 12.0, 2.3 Hz, 1H, H-6), 4.55 (d, *J* = 2.3 Hz, 1H, H-6a), 4.58 (dd, *J* = 12.0, 2.5 Hz, 1H, H-6), 6.05 (d, *J* = 2.0 Hz, 1H, H-8), 6.06 (d, *J* = 1.9 Hz, 1H, H-10), 6.48 (s, 1H, H-4), 6.49 (s, 1H, H-1), 4.72 (d, *J* = 9.7 Hz, 2H, C-6′H), 4.10-4.18 (m, 1H, C-5′H), 4.20-4.28 (m, 1H, C-4′H), 1.24 (s, 1H, OH-5′), 1.64 (s, 1H, NH-3′), 11.45 (s, 1H, OH-1′)	55.8 (OMe-9), 55.9 (OMe-3), 56.3 (OMe-2), 63.8 (C-6), 67.3 (C-12a), 75.7 (C-6a), 94.6 (C-8), 95.5 (C-10), 101.0 (C-4), 102.2 (C-1a), 109.1 (C-1), 142.1 (C-2), 148.2 (C-4a), 151.0 (C-3), 161.4 (C-7a), 164.2 (C-11), 167.4 (C-9), 195.0 (C-12), 44.6 (C-4′), 69.8 (C-5′), 69.3 (C-6′)

Table 8 Characterization the 6- deoxyclitoriacetal analogues (**A2**)

Compound	Name	Structure	MW.	^{1}H NMR	^{13}C NMR
A2	2-[2-Hydroxy-3-(12a-hydroxy-2,3,9-trimethoxy-12-oxo-6,6a,12,12a-tetrahydro-chromeno [3,4-*b*] chromen-11-yloxy)-propylamino]-propionic acid	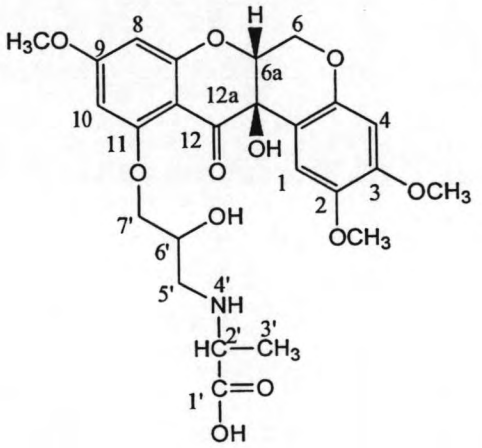	542.4 $[M+Na]^{+}$	3.71 (s, 3H, OMe-2), 3.76 (s, 3H, OMe-9), 3.79 (s, 3H, OMe-3), 4.45 (dd, J = 12.0, 2.3 Hz, 1H, H-6), 4.55 (d, J = 2.3 Hz, 1H, H-6a), 4.58 (dd, J = 12.0, 2.3 Hz, 1H, H-6), 6.04 (d, J = 1.9 Hz, 1H, H-8), 6.05 (d, J = 1.8 Hz, 1H, H-10), 6.47 (s, 1H, H-4), 6.49 (d, J = 7.4 Hz,1H, H-1), 4.76 (d, J = 11.0 Hz, 2H, C-7′H), 4.12-4.18 (m, 1H, C-6′H), 4.20-4.24 (m, 1H, C-5′H), 1.24 (s, 3H, C-3′H), 1.76 (s, 1H, NH-4′), 1.76 (s, 1H, OH-6′) 11.52 (s, 1H, OH-1′)	55.7 (OMe-9), 55.8 (OMe-3), 56.3 (OMe-2), 63.8 (C-6), 67.3 (C-12a), 75.7 (C-6a), 94.5 (C-8), 95.5 (C-10), 101.0 (C-4), 102.5 (C-1a), 109.2 (C-1), 144.0 (C-2), 148.1 (C-4a), 151.0 (C-3), 161.4 (C-7a), 163.5 (C-11), 167.3 (C-9), 191.0 (C-12), 44.7 (C-5′), 69.8 (C-6′), 69.3 (C-7′), 56.2 (C-2′), 167.3 (C-1′)

Table 9 Characterization the 6- deoxyclitoriacetal analogues (**A3**)

Compound	Name	Structure	MW.	^{1}H NMR	^{13}C NMR
A3	2-[2-Hydroxy-3-(12a-hydroxy-2,3,9-trimethoxy-12-oxo-6,6a,12,12a-tetrahydro-chromeno [3,4-*b*] chromen-11-yloxy)-propylamino]-3-methyl-pentanoic acid	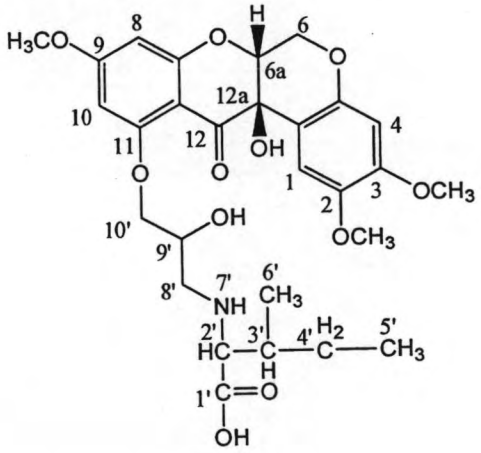	561.4 $[M]^{+}$	3.71 (s, 3H, OMe-2), 3.76 (s, 3H, OMe-9), 3.79 (s, 3H, OMe-3), 4.44 (dd, *J* = 12.0, 2.4 Hz, 1H, H-6), 4.54 (d, *J* = 2.3 Hz, 1H, H-6a), 4.57 (dd, *J* = 12.0, 2.4 Hz, 1H, H-6), 6.04 (d, *J* = 1.95 Hz, 1H, H-8), 6.05 (d, *J* = 1.74 Hz, 1H, H-10), 6.47 (s, 1H, H-4), 6.49 (d, *J* = 7.5 Hz,1H, H-1), 4.76 (d, *J* = 10.0 Hz, 2H, C-10′H), 4.14-4.18 (m, 1H, C-9′H), 4.20-4.23 (m, 1H, C-8′H), 0.87 (s, 3H, C-5′H), 1.24 (s, 2H, C-4′H), 1.81 (s, 1H, NH-4′), 1.81 (s, 1H, OH-9′) 2.03 (s, 1H, C-3′H), 3.58 (s, 1H, C-2′H)	55.8 (OMe-9), 55.9 (OMe-3), 56.3 (OMe-2), 63.8 (C-6), 67.3 (C-12a), 75.7 (C-6a), 94.5 (C-8), 95.5 (C-10), 101.0 (C-4), 102.5 (C-1a), 109.1 (C-1), 144.0 (C-2), 148.0 (C-4a), 151.0 (C-3), 161.4 (C-7a), 163.5 (C-11), 167.3 (C-9), 190.5 (C-12), 44.7 (C-8′), 69.8 (C-9′), 69.3 (C-10′), 56.2 (C-2′), 163.5 (C-1′)

Table 10 Characterization the 6- deoxyclitoriacetal analogues (**A4**)

Compound	Name	Structure	MW.	^{1}H NMR	^{13}C NMR
A4	2-[2-Hydroxy-3-(12a-hydroxy-2,3,9-trimethoxy-12-oxo-6,6a,12,12a-tetrahydro-chromeno [3,4-*b*] chromen-11-yloxy)-propylamino]-3-mercapto-propionic acid	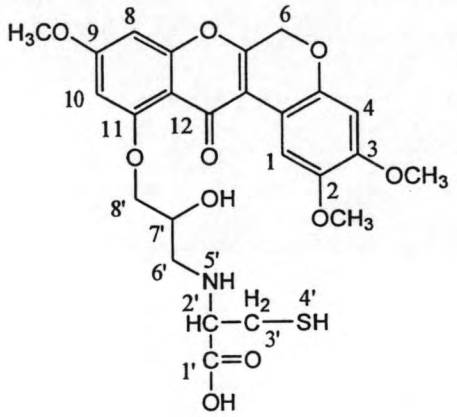	571.5 $[M+K]^{+}$	3.66 (s, 3H, OMe-2), 3.71 (s, 3H, OMe-9), 3.74 (s, 3H, OMe-3), 4.38 (dd, J = 12.0, 2.3 Hz, 1H, H-6), 4.48 (d, J = 2.3 Hz, 1H, H-6a), 4.52 (dd, J = 12.0, 2.3 Hz, 1H, H-6), 5.98 (d, J = 2.0 Hz, 1H, H-8), 5.99 (d, J = 2.0 Hz, 1H, H-10), 6.42 (s, 1H, H-4), 6.44 (s, 1H, H-1), 4.64 (d, J = 9.7 Hz, 2H, C-8′H), 4.04-4.11 (m, 1H, C-7′H), 4.13-4.19 (m, 1H, C-6′H), 3.55 (s, 1H, C-2′H), 1.20 (s, 1H, SH-4′), 1.60 (s, 1H, NH-5′), 11.44 (s, 1H, OH-1′)	55.8 (OMe-9), 55.9 (OMe-3), 56.3 (OMe-2), 63.8 (C-6), 67.3 (C-12a), 75.7 (C-6a), 94.5 (C-8), 95.5 (C-10), 101.0 (C-4), 102.5 (C-1a), 109.1 (C-1), 144.0 (C-2), 148.0 (C-4a), 151.0 (C-3), 161.4 (C-7a), 163.5 (C-11), 167.3 (C-9), 190.5 (C-12), 44.7 (C-6′), 69.8 (C-7′), 69.3 (C-8′), 56.2 (C-2′), 163.5 (C-1′)

Table 11 Characterization the 6- deoxyclitoriacetal analogues (**A5**)

Compound	Name	Structure	MW.	^{1}H NMR	^{13}C NMR
A5	5-Guanidino-2-[2-Hydroxy-3-(12a-hydroxy-2,3,9-trimethoxy-12-oxo-6,6a,12,12a-tetrahydro-chromeno [3,4-*b*] chromen-11-yloxy)-propylamino]-pentanoic acid	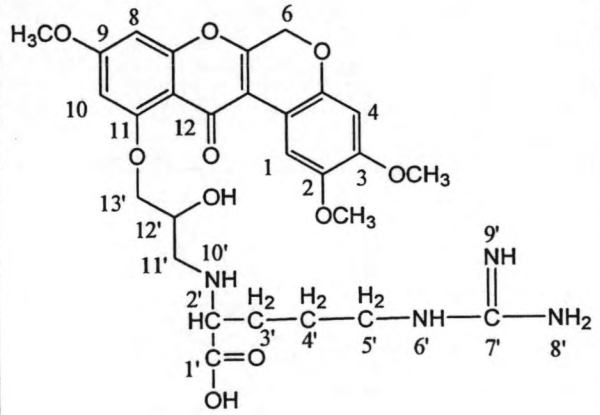	625.8 $[M+K]^{+}$	3.71 (s, 3H, OMe-2), 3.76 (s, 3H, OMe-9), 3.79 (s, 3H, OMe-3), 4.45 (dd, J = 12.0, 2.3 Hz, 1H, H-6), 4.54 (d, J = 2.3 Hz, 1H, H-6a), 4.58 (dd, J = 12.0, 2.3 Hz, 1H, H-6), 6.04 (d, J = 1.9 Hz, 1H, H-8), 6.05 (d, J = 1.7 Hz, 1H, H-10), 6.47 (s, 1H, H-4), 6.48 (d, J = 7.4 Hz, 1H, H-1), 4.75 (d, J = 7.1 Hz, 2H, C-13′H), 4.09-4.17 (m, 1H, C-12′H), 4.20-4.24 (m, 1H, C-11′H), 2.03 (s, 2H, C-4′H), 2.47 (s, 2H, C-5′H), 1.24 (s, 2H, C-3′H), 1.78 (s, 1H, NH-10′), 3.60 (s, 1H, C-2′H)11.52 (s, 1H, OH-1′)	55.8 (OMe-9), 55.9 (OMe-3), 56.3 (OMe-2), 63.8 (C-6), 67.3 (C-12a), 75.7 (C-6a), 94.5 (C-8), 95.5 (C-10), 101.0 (C-4), 102.5 (C-1a), 109.1 (C-1), 144.0 (C-2), 148.0 (C-4a), 151.0 (C-3), 161.4 (C-7a), 163.5 (C-11), 167.3 (C-9), 190.5 (C-12), 44.7 (C-11′), 69.8 (C-12′), 69.3 (C-13′), 56.2 (C-3′), 163.5 (C-1′)

3.4.2 The 6-deoxyclitoriacetal – pyrimidine base analogues

In general, the major target for many anticancer drugs is deoxyribonucleic acid (DNA). It is a long polymer made from repeating units called nucleotides. Pyrimidine base is one of the nucleotide components. Pyrimidines include the base cytosine, thymine and uracil, which are components of DNA and RNA. Pyrimidine analog was used as a drug in the treatment of cancer. It belongs to the family of drugs called antimetabolites [53]. Pyrimidine is a nitrogenous heterocyclic base. The nitrogen atoms in heterocyclic base may increase the stability of the complex through forming hydrogen bonds with DNA. Therefore, in this work the structure of 6-deoxyclitoriacetal were modified with certain pyrimidine base. In order to study the effect of functional groups on pyrimidine base to the cytotoxicity, three pyrimidine bases were chosen to synthesize with 6-deoxyclitoriacetal namely cytosine, thymine and uracil. Compound **B** is a tosylate derivative of 6-deoxyclitoriacetal. Compounds **B1** to **B3** are the products of replacing the tosylate derivative with the pyrimidine base mentioned above. The reaction scheme was shown in Scheme 17. The details of the spectroscopy characterization including ^{1}H-NMR, ^{13}C-NMR and LC-ESI mass spectroscopy for all the compounds were given in Table 12 to 15.

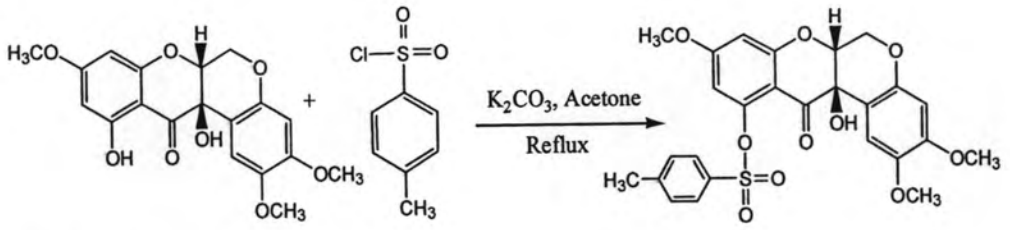

6-deoxyclitoriacetal toluene-4-sulfonyl chloride **B**

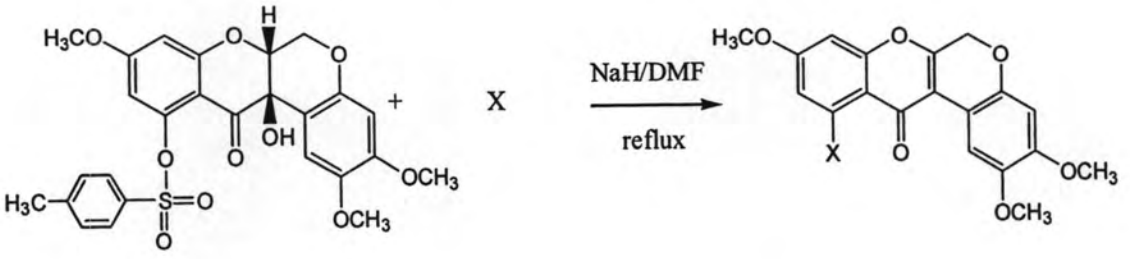

B **B1-B3**

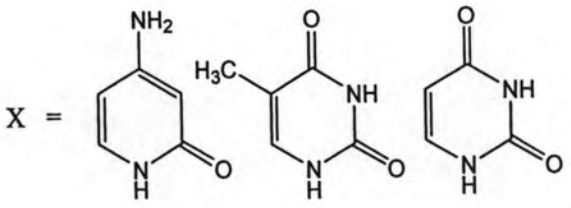

cytosine thymine uracil

B1 **B2** **B3**

Scheme 17 Synthesis pathway for compounds **B, B1** to **B3**

Table 12 Characterization the 6- deoxyclitoriacetal analogues (**B**)

Compound	Name	Structure	MW.	^{1}H NMR	^{13}C NMR
B	Toluene-4-sulfonic acid 12a-hydroxy-2,3,9-trimethoxy-12-oxo-6,6a,12,12a-tetrahydrochromeno[3,4-*b*]chromen-11-yl ester	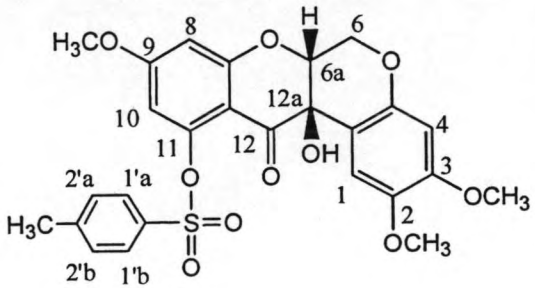	550.4 $[M+Na]^{+}$	3.68 (s, 3H, OMe-2), 3.77 (s, 3H, OMe-9), 3.80 (s, 3H, OMe-3), 4.48 (dd, J = 12.2, 2.3 Hz, 1H, H-6), 4.53 (d, J = 2.0 Hz, 1H, H-6a), 4.57 (dd, J = 12.2, 2.3 Hz, 1H, H-6), 6.03 (d, J = 2.3 Hz, 1H, H-8), 6.32 (d, J = 2.3 Hz, 1H, H-10), 6.47 (s, 1H, H-4), 6.66 (s, 1H, H-1), 7.89 (d, J = 8.2, 1H, C1′-Ha), 7.91 (d, J = 8.2 Hz, 1H, C1′-Hb), 7.38 (d, J = 8.13, 1H, C2′-Ha), 7.34 (d, J = 8.13 Hz, 1H, C2′-Hb), 2.47 (s, 3H, C3′)	55.6 (OMe-9), 55.8 (OMe-3), 56.4 (OMe-2), 63.8 (C-6), 67.1 (C-12a), 75.7 (C-6a), 94.0 (C-8), 94.5 (C-10), 101.0 (C-4), 102.2 (C-1a), 109.4 (C-1), 142.1 (C-2), 148.2 (C-4a), 151.0 (C-3), 161.4 (C-7a), 164.2 (C-11), 168.8 (C-9), 195.0 (C-12), 20.9 (C1′), 128.0 (C-2′a), 128.0 (C-2′b), 130.0 (C-3′a), 130.0 (C-3′b)

Table 13 Characterization the 6- deoxyclitoriacetal analogues (**B1**)

Compound	Name	Structure	MW.	^{1}H NMR	^{13}C NMR
B1	4-Amino-1-(2,3,9-trimethoxy-12-oxo-6,12-dihydro-chromeno [3,4-*b*] chromen-11-yl)-1*H*-pyridin-2-one	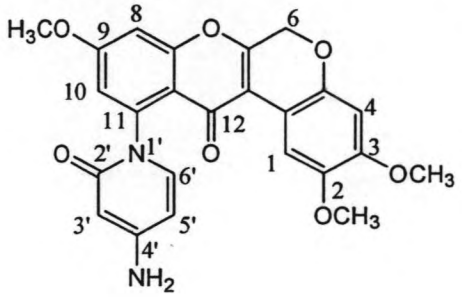	449.0 $[M+H]^{+}$	3.68 (s, 3H, OMe-2), 3.75 (s, 3H, OMe-9), 3.80 (s, 3H, OMe-3), 4.42 (dd, J = 12.0, 2.5 Hz, 1H, H-6), 4.59 (dd, J = 12.0, 2.5 Hz, 1H, H-6), 5.96 (d, J = 2.3 Hz, 1H, H-8), 6.00 (d, J = 2.2 Hz, 1H, H-10), 6.48 (s, 1H, H-4), 6.60 (s, 1H, H-1), 2.46 (s, 1H, H-4′), 5.27 (s, 1H, H-5′), 5.98 (s, 1H, H-3′), 7.37 (d, J = 8.1 Hz, 1H, H-6′)	55.6 (OMe-9), 55.8 (OMe-3), 56.4 (OMe-2), 63.8 (C-6), 67.1 (C-12a), 75.7 (C-6a), 94.0 (C-8), 94.5 (C-10), 101.0 (C-4), 102.2 (C-1a), 109.4 (C-1), 142.1 (C-2), 148.2 (C-4a), 151.0 (C-3), 161.4 (C-7a), 164.2 (C-11), 168.8 (C-9), 195.0 (C-12)

Table 14 Characterization the 6- deoxyclitoriacetal analogues (**B2**)

Compound	Name	Structure	MW.	^{1}H NMR	^{13}C NMR
B2	1-(12a-Hydroxy-2,3,9-trimethoxy-12-oxo-6,6a,12,12a-tetrahydro-chromeno [3,4-*b*] chromen-11-yl)-5-methyl-1*H*-pyrimidine-2,4-dione	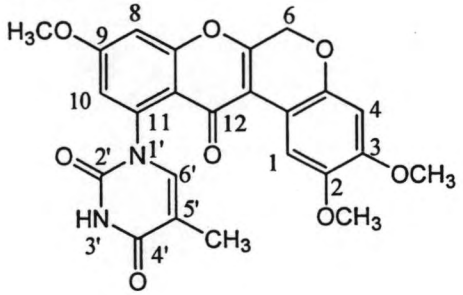	487.4 $[M+Na]^{+}$	3.68 (s, 3H, OMe-2), 3.75 (s, 3H, OMe-9), 3.80 (s, 3H, OMe-3), 4.42 (dd, J = 12.0, 2.5 Hz, 1H, H-6), 4.51 (d, J = 1.89 Hz, 1H, H-6a), 4.59 (dd, J = 12.0, 2.5 Hz, 1H, H-6), 5.96 (d, J = 2.2 Hz, 1H, H-8), 6.00 (d, J = 2.2 Hz, 1H, H-10), 6.48 (s, 1H, H-4), 6.61 (s, 1H, H-1), 2.47 (s, 3H, H-5′), 7.39 (s, 1H, H-6′), 11.52 (s, 1H, H-3′)	55.8 (OMe-9), 56.4 (OMe-3), 56.5 (OMe-2), 63.8 (C-6), 67.4 (C-12a), 75.7 (C-6a), 94.4 (C-8), 95.3 (C-10), 101.0 (C-4), 102.6 (C-1a), 109.5 (C-1), 142.3 (C-2), 148.3 (C-4a), 151.1 (C-3), 161.4 (C-7a), 162.6 (C-11), 168.8 (C-9), 195.0 (C-12),

Table 15 Characterization the 6- deoxyclitoriacetal analogues (**B3**)

Compound	Name	Structure	MW.	^{1}H NMR	^{13}C NMR
B3	1-(12a-Hydroxy-2,3,9-trimethoxy-12-oxo-6,6a,12,12a-tetrahydro-chromeno [3,4-*b*] chromen-11-yl)-1*H*-pyridine-2,4-dione	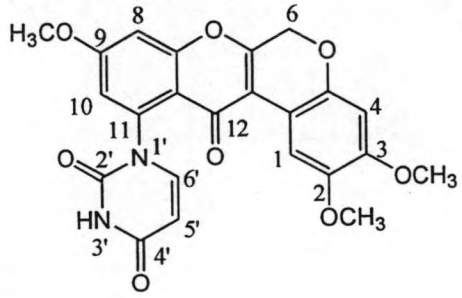	472.2 $[M+Na]^{+}$	3.68 (s, 3H, OMe-2), 3.75 (s, 3H, OMe-9), 3.80 (s, 3H, OMe-3), 4.42 (dd, J = 12.0, 2.5 Hz, 1H, H-6), 4.50 (d, J = 2.0 Hz, 1H, H-6a), 4.57 (dd, J = 12.0, 2.5 Hz, 1H, H-6), 5.96 (d, J = 2.14 Hz, 1H, H-8), 6.00 (d, J = 1.95 Hz, 1H, H-10), 6.48 (s, 1H, H-4), 6.60 (s, 1H, H-1)	55.6 (OMe-9), 55.8 (OMe-3), 56.4 (OMe-2), 63.8 (C-6), 67.1 (C-12a), 75.7 (C-6a), 94.0 (C-8), 94.5 (C-10), 101.0 (C-4), 102.2 (C-1a), 109.4 (C-1), 142.1 (C-2), 148.2 (C-4a), 151.0 (C-3), 161.4 (C-7a), 164.2 (C-11), 168.8 (C-9), 195.0 (C-12),

3.4.3 The 6-deoxyclitoriacetal – aromatic carboxylic analogues

In terms of structure-activity relationships, the introduction of bulky groups in the moleucle, as exemplified with phenyl-analogs, generally reducing cytotoxicity, but substitution with short chain or small molecules can help the forming of hydrogen bonding with DNA base pairs including amine groups potentiated the cytotoxic activity [54]. Therefore, in this work the structure of 6-deoxyclitoriacetal were modified with phenyl analogs by substitution with different small molecules. In order to study the effect of functional group on aromatic carboxylic compound to the cytotoxicity, five aromatic carboxylic compounds were chosen to synthesize with 6-deoxyclitoriacetal namely, 4-*tert*-butylbenzoic acid, benzoic acid, 4-chlorobenzoic acid, 4-hydroxybenzoic acid and 4-aminobenzoic acid. Compounds **C** to **G** are the products of the reaction. The reaction scheme was shown in Scheme 18. The details of the spectroscopy characterization including ^{1}H-NMR, ^{13}C-NMR and LC-ESI mass spectroscopy for all the compounds were given in Table 16 to 20.

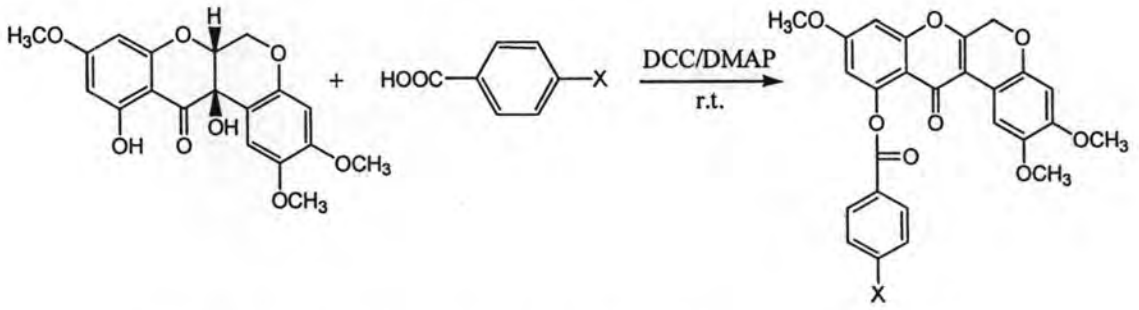

6-deoxyclitoriacetal aromatic carboxylic acid **C-G**

C, X = 4-tert-butyl; **D**, X = H; **E**, X = Cl; **F**, X = OH; **G**, X = NH_2

Scheme 18 Synthesis pathway for compounds **C** to **G**

Table 16 Characterization the 6- deoxyclitoriacetal analogues (**C**)

Compound	Name	Structure	MW.	^{1}H NMR	^{13}C NMR
C	4-*tert*-butyl-benzoic acid 12a-hydroxy-2,3,9-trimethoxy-12-oxo-6,6a,12,12a-tetrahydro-chromeno[3,4-*b*]chromen-11-yl ester	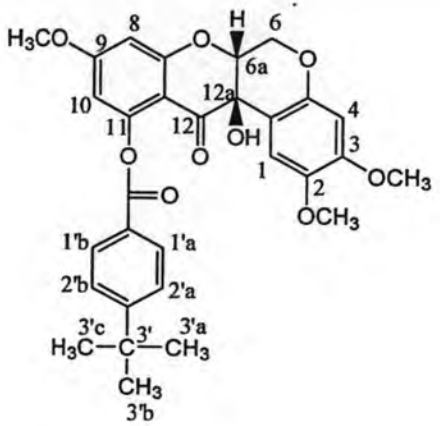	574.4 $[M+Na]^{+}$	3.79 (s, 3H, OMe-2), 3.81 (s, 3H, OMe-9), 3.84 (s, 3H, OMe-3), 4.48 (dd, J = 11.4, 2.5 Hz, 1H, H-6), 4.44 (d, J = 1.8 Hz, 1H, H-6a), 4.60 (dd, J = 10.4, 2.5 Hz, 1H, H-6), 6.33 (d, J = 2.3 Hz, 1H, H-8), 6.36 (d, J = 2.5 Hz, 1H, H-10), 6.43 (s, 1H, H-4), 6.47 (s, 1H, H-1), 7.56 (d, J = 8.4, 1H, C1′-Ha), 7.58 (d, J = 8.4 Hz, 1H, C1′-Hb), 8.12 (d, J = 8.4, 1H, C2′-Ha), 8.14 (d, J = 8.4 Hz, 1H, C2′-Hb), 1.59 (s, 9H, C3′a,C3′b,C′3c)	55.6 (OMe-9), 55.8 (OMe-3), 56.4 (OMe-2), 63.8 (C-6), 67.1 (C-12a), 75.7 (C-6a), 94.0 (C-8), 94.5 (C-10), 101.0 (C-4), 102.2 (C-1a), 109.4 (C-1), 142.1 (C-2), 148.2 (C-4a), 151.0 (C-3), 161.4 (C-7a), 164.2 (C-11), 168.8 (C-9), 195.0 (C-12), 125.8 (C-2′a), 125.8 (C-2′b), 31.5 (C-3′a) 31.5 (C-3′b) 31.5 (C-3′c)

Table 17 Characterization the 6- deoxyclitoriacetal analogues (**D**)

Compound	Name	Structure	MW.	^{1}H NMR	^{13}C NMR
D	benzoic acid 12a-hydroxy-2,3,9-trimethoxy-12-oxo-6,6a,12,12a-tetrahydro-chromeno[3,4-*b*]chromen-11-yl ester	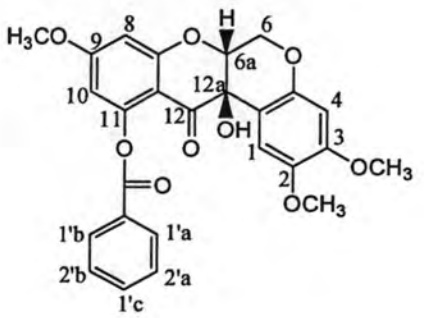	533.3 $[M+K]^{+}$	3.78 (s, 3H, OMe-2), 3.80 (s, 3H, OMe-9), 3.83 (s, 3H, OMe-3), 4.46 (dd, J = 10.9, 2.3 Hz, 1H, H-6), 4.57 (d, J = 2.0 Hz, 1H, H-6a), 4.60 (dd, J = 9.1, 2.3 Hz, 1H, H-6), 6.33 (d, J = 2.3 Hz, 1H, H-8), 6.36 (d, J = 2.5 Hz, 1H, H-10), 6.48 (s, 1H, H-4), 6.69 (s, 1H, H-1), 8.09 (d, J = 7.7, 1H, C1′-Ha), 8.19 (d, J = 7.7 Hz, 1H, C1′-Hb), 8.22 (d, J = 7.7 Hz, 1H, C1′-Hc), 7.55 (d, J = 7.5, 1H, C2′-Ha), 7.57 (d, J = 7.5 Hz, 1H, C2′-Hb)	55.8 (OMe-9), 55.9 (OMe-3), 56.3 (OMe-2), 63.6 (C-6), 66.9 (C-12a), 75.6 (C-6a), 94.5 (C-8), 95.6 (C-10), 100.1 (C-4), 101.1 (C-1a), 109.3 (C-1), 144.0 (C-2), 148.3 (C-4a), 151.3 (C-3), 161.6 (C-7a), 164.3 (C-11), 169.0 (C-9), 195.1 (C-12),

Table 18 Characterization the 6- deoxyclitoriacetal analogues (**E**)

Compound	Name	Structure	MW.	^{1}H NMR	^{13}C NMR
E	4-chloro-benzoic acid 2,3,9-trimethoxy-12-oxo-6,12-dihydro-chromeno[3,4-*b*]chromen-11-yl ester	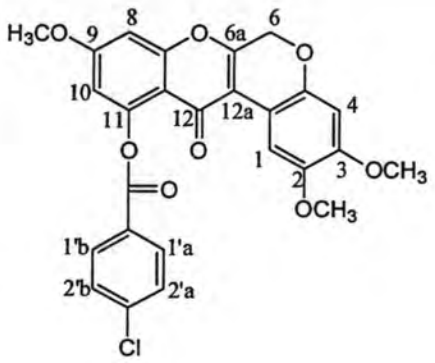	535.3 $[M+Na]^{+}$	3.79 (s, 3H, OMe-2), 3.81 (s, 3H, OMe-9), 3.81 (s, 3H, OMe-3), 4.48 (dd, J = 11.2, 2.1 Hz, 1H, H-6), 4.60 (dd, J = 9.9, 2.4 Hz, 1H, H-6), 6.35 (d, J = 2.3 Hz, 1H, H-8), 6.36 (d, J = 2.3 Hz, 1H, H-10), 6.39 (s, 1H, H-4), 6.45 (s, 1H, H-1), 7.52 (d, J = 8.5, 1H, C1′-Ha), 7.55 (d, J = 8.5 Hz, 1H, C1′-Hb), 8.14 (d, J = 8.5 Hz, 1H, C2′-Ha), 8.16 (d, J = 8.5, 1H, C2′-Hb)	55.8 (OMe-9), 55.9 (OMe-3), 56.3 (OMe-2), 63.6 (C-6), 66.9 (C-12a), 75.6 (C-6a), 94.5 (C-8), 95.6 (C-10), 100.1 (C-4), 101.1 (C-1a), 109.3 (C-1), 144.0 (C-2), 148.3 (C-4a), 151.3 (C-3), 161.6 (C-7a), 164.3 (C-11), 169.0 (C-9), 195.1 (C-12),

Table 19 Characterization the 6- deoxyclitoriacetal analogues (**F**)

Compound	Name	Structure	MW.	^{1}H NMR	^{13}C NMR
F	4-hydroxy-benzoic acid 2,3,9-trimethoxy-12-oxo-6,12-dihydro-chromeno[3,4-*b*]chromen-11-yl ester	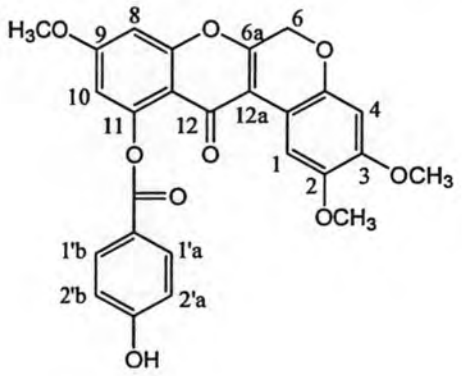	531.2 $[M+K]^{+}$	3.75 (s, 3H, OMe-2), 3.77 (s, 3H, OMe-9), 3.81 (s, 3H, OMe-3), 4.45 (dd, J = 12.0, 2.5 Hz, 1H, H-6), 4.59 (dd, J = 12.0, 2.5 Hz, 1H, H-6), 5.97 (d, J = 2.2 Hz, 1H, H-8), 6.05 (d, J = 2.2 Hz, 1H, H-10), 6.5 (s, 1H, H-4), 6.7 (s, 1H, H-1), 7.27 (d, J = 8.1, 1H, C1′-Ha), 7.29 (d, J = 8.1 Hz, 1H, C1′-Hb), 8.0 (d, J = 8.15 Hz, 1H, C2′-Ha), 8.02 (d, J = 8.15, 1H, C2′-Hb)	55.8 (OMe-9), 55.9 (OMe-3), 56.3 (OMe-2), 63.6 (C-6), 66.9 (C-12a), 75.6 (C-6a), 94.5 (C-8), 95.6 (C-10), 100.1 (C-4), 101.1 (C-1a), 109.3 (C-1), 144.0 (C-2), 148.3 (C-4a), 151.3 (C-3), 161.6 (C-7a), 164.3 (C-11), 169.0 (C-9), 195.1 (C-12)

Table 20 Characterization the 6- deoxyclitoriacetal analogues (**G**)

Compound	Name	Structure	MW.	^{1}H NMR	^{13}C NMR
G	4-amino-benzoic acid 2,3,9-trimethoxy-12-oxo-6,12-dihydro-chromeno[3,4-*b*]chromen-11-yl ester	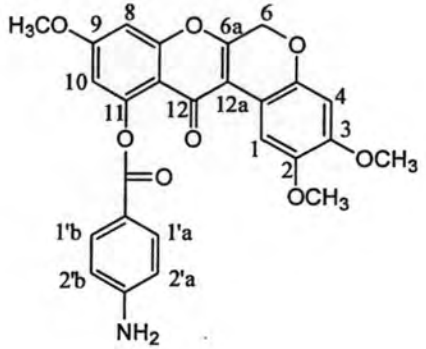	492.8 $[M+2H]^{+}$	3.76 (s, 3H, OMe-2), 3.79 (s, 3H, OMe-9), 3.82 (s, 3H, OMe-3), 4.44 (dd, J = 11.2, 4.5 Hz, 1H, H-6), 4.58 (dd, J = 11.2, 4.5 Hz, 1H, H-6), 6.30 (d, J = 2.3 Hz, 1H, H-8), 6.34 (d, J = 2.3 Hz, 1H, H-10), 6.43 (s, 1H, H-4), 6.46 (s, 1H, H-1), 7.40 (d, J = 8.6, 1H, C1′-Ha), 7.42 (d, J = 8.6 Hz, 1H, C1′-Hb), 7.97 (d, J = 8.6 Hz, 1H, C2′-Ha), 7.99 (d, J = 8.6, 1H, C2′-Hb)	55.8 (OMe-9), 55.9 (OMe-3), 56.3 (OMe-2), 63.6 (C-6), 66.9 (C-12a), 75.6 (C-6a), 94.5 (C-8), 95.6 (C-10), 100.1 (C-4), 101.1 (C-1a), 109.3 (C-1), 144.0 (C-2), 148.3 (C-4a), 151.3 (C-3), 161.6 (C-7a), 164.3 (C-11), 169.0 (C-9), 195.1 (C-12)

3.5 Cytotoxic activities of 6-deoxyclitoriacetal and its analogues

In this research, the cytotoxic activities of 6-deoxyclitoriacetal and its analogues were studies to investigate the structure-activity relationship. As mentioned in the previous section, we propose that important factors for 6-deoxyclitoriacetal to have good cytotoxicity are (i) at lease one part of the molecule should be planar (to intercalate part with DNA), (ii) the molecule adopts a bent shape or V shape (to stabilize the intercalation by locking a part of molecule in the minor or major groove of a DNA double strand) and the last factor is (iii) the molecule should have functional groups that can participate hydrogen bonding to base pairs of DNA double strand (to enhance the stability of deformed DNA, leading to inhibit the duplicate of DNA). Therefore, the derivatives of 6-deoxyclitoriacetal were synthesis to study the above mentioned factors, and then tested for their cytotoxicities.

All synthesized compounds (**A**, **A1** to **A5**, **B**, **B1** to **B3**, **C** to **G**) were tested for cytotoxicity against KB (Human mouth carcinoma), MCF7 (Breast cancer) and NCL-H187 (Human small lung cancer) cell lines. Doxorubicin and ellipticine were used as the positive control for this cytotoxic activity assay. The cytotoxic activities of 6-deoxyclitoriacetal (**1**), stemonal (**2**) and their 6-deoxyclitoriacetal analogues were reported in IC_{50} value. The IC_{50} is the half maximal (50%) inhibitory concentration (IC) of a substance. In general, higher IC_{50} means lower cytotoxic activity. The cytotoxic activity results of all compounds were tabulated in Table 21.

Table 21 Cytotoxic activities of 6-deoxyclitoriacetal (**1**), stemonal (**2**) and 6-deoxyclitoriacetal analogues (**A**, **A1** to **A5**, **B**, **B1** to **B3**, **C** to **G**) against KB (Human mouth carcinoma), MCF7 (Breast cancer) and NCL-H187 (Human small lung cancer) cell lines.

Compound	IC_{50} (μg/ml)		
	KB	MCF7	NCl-H187
doxorubicin	0.325	0.822	0.041
ellipticine	0.147	Inactive	0.441
6-deoxyclitoriacetal **(1)**	0.08	0.26	0.04
Stemonal **(2)**	Inactive	Inactive	Inactive
A	2.87	7.33	3.21
A1	23.22	Inactive	20.74
A2	35.54	25.61	3.31
A3	5.05	18.57	6.01
A4	Inactive	Inactive	Inactive
A5	1.45	38.45	Inactive
B	0.017	Inactive	0.018
B1	18.65	Inactive	11.61
B2	25.39	Inactive	11.61
B3	1.45	Inactive	0.255
C	Inactive	Inactive	Inactive
D	40.21	Inactive	22.50
E	32.06	Inactive	19.13
F	47.83	Inactive	27.29
G	2.64	Inactive	8.28

Doxorubicin (Adriamycin) is a commercial drug, generally used in cancer chemotherapy (Fig. 27). It is an anthracycline antibiotic. It can intercalate into base pairs of DNA. This manner likes all anthracyclines. It is commonly used to treat some leukemia as well as cancers of the breast, lung, stomach, bladder, ovaries and others [1, 2]. Doxorubicin is known to interact with DNA by intercalation and then inhibit the progression of the topoisomerase II, enzyme that unwinds DNA for transcription. The planar aromatic chromophore moiety intercalates between two base pairs of the DNA, while the six-member daunosamine sugar sits in the minor groove and interacts with base pairs adjacent to the intercalation site [2].

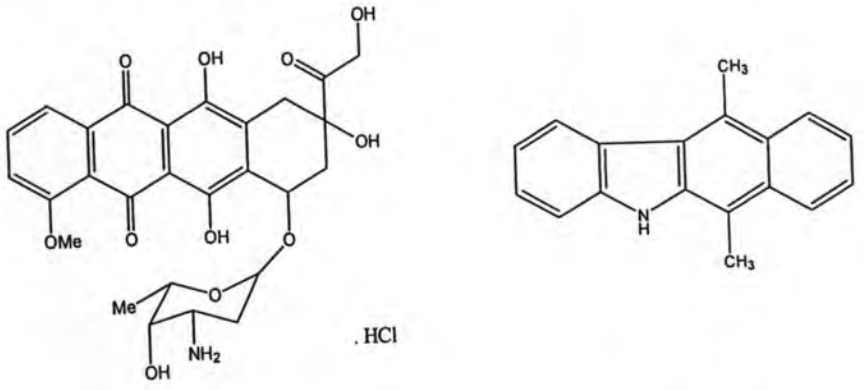

(a) (b)

Fig. 27 Chemical structures of (a) doxorubicin HCl and (b) ellipticine

Ellipticine exhibits significant antitumor and anti-HIV activities [55]. It is highly efficienct against several types of cancer and has rather limited toxic side effects [56]. Ellipticine is an antineoplastic agent (Fig. 27), the mode of action of which was considered to be based mainly on DNA intercalation and/or inhibition of topoisomerase II [55, 56].

Two positive control drugs have cytotoxic activities against three cancer cell lines, i.e. KB (Human mouth carcinoma), MCF7 (Breast cancer) and NCL-H187 (Human small lung cancer). For doxorubicin, the results indicate significant cytotoxic activities with the IC_{50} value of 0.325, 0.822 and 0.041 μg/ml against KB, MCF7 and NCI-H187, respectively. While, ellipticine is active towards only two cancer cell lines, i.e. KB and NCI-H187, with the IC_{50} value of 0.147 and 0.441 μg/ml, respectively, but it is inactive in the MCF7 assay.

The cytotoxic activities of **1** (Fig. 28) showed the IC_{50} value of 0.08, 0.26 and 0.04 μg/ml. In contrast, **2** (Fig. 28) showed inactive activity for all tested cell lines These results reveal that **1** have good cytotoxic activities when compared to that of doxorubicin and ellipticine.

Compound **1** has the similar structure to doxorubicin HCl. It adopts the planar molecule at ring AB and CD and has a bending part at C6a-C12a, causing **1** to have good cytotoxic activities against the three cell lines. In contrast, the compound **2** adopt a planar structure; it showed the inactive cytotoxic activities.

It can be deduced that being a planar aromatic molecule is although important for intercalation but not the only factor for having good cytotoxicity. It is crutial that the drug-DNA complex must be stabilized intercalating site. This is possible if the molecule has a bent shape, with the body part intercalating into the DNA and the bending tail part having intermolecular interaction such as hydrogen bonding or pi-pi interaction with base pairs adjacent to the intercalating site.

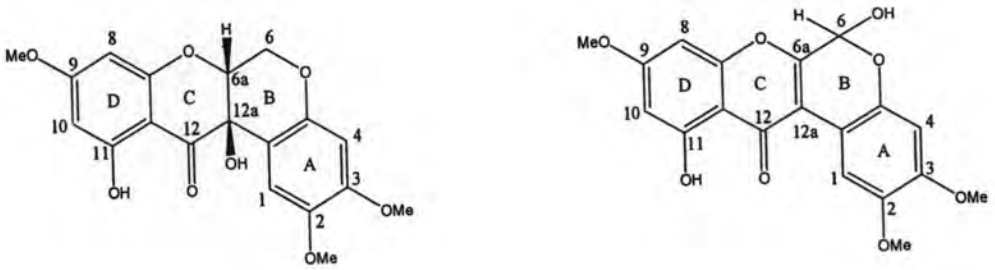

(a) (b)

Fig. 28 Chemical structures of (a) 6-deoxyclitoriacetal (**1**), (b) stemonal (**2**),

The results of the cytotoxic activity of 6-deoxyclitoriacetal and stemenal are consistent with the spectroscopic data of the substance-DNA intercalation ability. In order to enhance the anticancer activity by improving the binding ability or stabilizing intercalation with DNA, 6-deoxyclitoriacetal analogues were prepared by extending the functional group at C11-OH. The preferred functional groups are flexible functional groups with strong hydrogen bonding to the base pairs of DNA to help

stabilization of the substance-DNA intercalation, for example, amino acid, aromatic carboxylic acid and pyrimidine base.

3.5.1 6-deoxyclitoriacetal – amino acid analogues

In order to study the effect of a functional group of amino acid and the effect of their side chain-lengths on cytotoxicity, five amino acids were selected to be synthesized with 6-deoxyclitoriacetal, namely glycine, alanine, isoleucine, cystein and arginine. Compound **A** is the epoxide derivative of 6-deoxyclitoriacetal. Compounds **A1** to **A5** are the products of the epoxide ring-opening of 6-deoxyclitoriacetal with amino acids mentioned above. All compounds were tested for the cytotoxicity against KB (Human mouth carcinoma), MCF7 (Breast cancer) and NCL-H187 (Human small lung cancer) cell lines. The cytotoxic activities results of each compound were demonstrated as follows,

The compound **A** (Fig. 29a) has the epoxy ring at C11 of **1**. The structure has a bent shape at C6a-C12a. It showed strong cytotoxicity against KB, MCF7 and NCI-H187 with the IC_{50} value of 2.87, 7.33 and 3.21 μg/ml, respectively. These results consistent with the previously reported cytotoxicity of 2′,3′-epoxypropoxy substituted xanthones that efficiently prohibit growth of cancer cells via intercalation of xanthone group into DNA base pair and alkylation of epoxide by N-7 guanine in the presence of topoisomerase II [57, 58].

Compound **A1** (Fig. 29b) is the product of the epoxide ring opening of **A** with glycine. The structure adopts a bent shape at C6a-C12a. It exhibited moderate cytotoxicity against KB and NCI-H187 with the IC_{50} value of 23.22 and 20.74 μg/ml, respectively, but showed the inactive activity in MCF7 cell line.

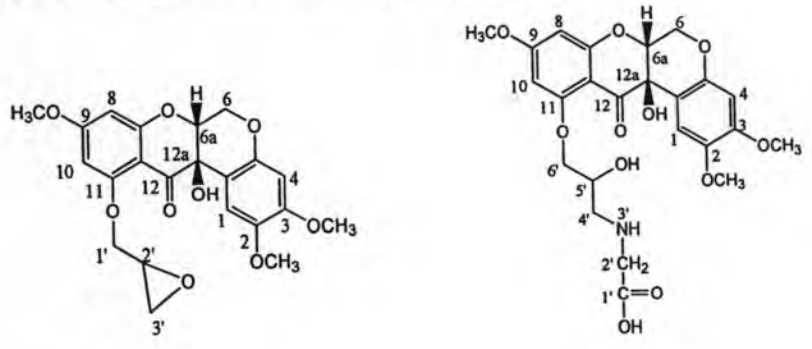

(a) (b)

Fig. 29 The chemical structures of compound (a) **A**, (b) **A1**

Compound **A2** (Fig. 30a) is the product of the epoxide ring opening of **A** with alanine. The structure also has a bent shape at C6a-C12a. It exhibited moderate cytotoxicity against KB and MCF7 with the IC_{50} value of 35.54 and 25.61 μg/ml, respectively, but showed strong cytotoxicity toward the NCI-H187 cell line with the IC_{50} value of 3.31 μg/ml.

Compound **A3** (Fig. 30b) is the product of the epoxide ring opening of **A** with isoluecine. The structure adopts the same bent shape at C6a-C12a as compound **A1** and **A2**. It was active against three cancer cell lines. Interestingly, it showed strong cytotoxicity against KB and NCI-H187 with the IC_{50} value of 5.05 and 6.01 μg/ml, respectively, but exhibited moderate cytotoxicity against the MCF7 cell line with the IC_{50} value of 18.57 μg/ml.

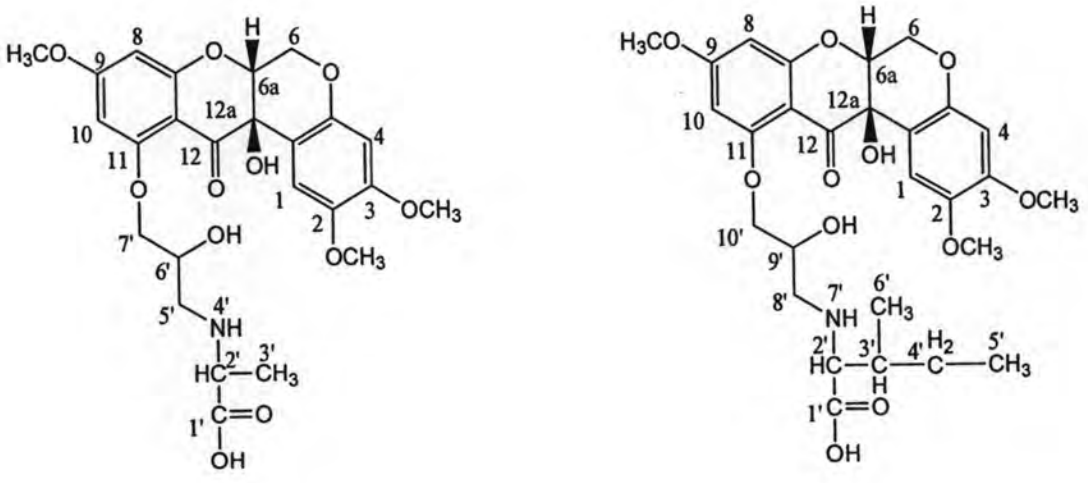

(a) (b)

Fig. 30 The chemical structure of compound (a) **A2**, (b) **A3**

As a result, **A1, A2** and **A3** all adopt a bent shape at C6a-C12a. For KB cancer cell lines, **A1** had more cytotoxic activity than **A2** and showed the IC_{50} value of 23.22 and 35.54 μg/ml, respectively. However, the compound **A3** was found to be strongly active against this cell line with the IC_{50} value of 5.05 μg/ml. In addition, **A3** had potential cytotoxic activity against MCF7 cell lines with the IC_{50} value of 18.57 μg/ml. It was better than in both **A1** and **A2**. For NCI-H187 cell line, **A2** was strongly selective with the IC_{50} value of 3.31 μg/ml. However, **A3** still have potential

cytotoxic activity with NCI-H187 cell line and better than that of **A1**. It can be concluded that the longer aliphatic chain in **A1**, **A2** and **A3**, showed higher cytotoxic activities against both KB and MCF7 cell lines.

Compound **A4** (Fig. 31a) is the product of the epoxide ring opening of **A** with cystein. The data from mass spectrum demonstrated that **A4** has no bent shape at C6a-C12a, therefore, it is a planar structure. This compound was inactive against three cancer cell lines. This results consistent with our hypothesis that the molecule with a good cytotoxicity should adopt a bent shape.

Compound **A5** (Fig. 31b) is the product of the epoxide ring opening of **A** with arginine. It is similar structure to **A4** at C6a-C12a so it adopts a planar structure. This compound exhibited strong cytotoxicity against KB cell line with the IC_{50} value of 1.45 μg/ml and moderate cytotoxicity against MCF7 cell line with the IC_{50} value of 38.45 μg/ml but it was inactive toward the NCI-H187 cell line.

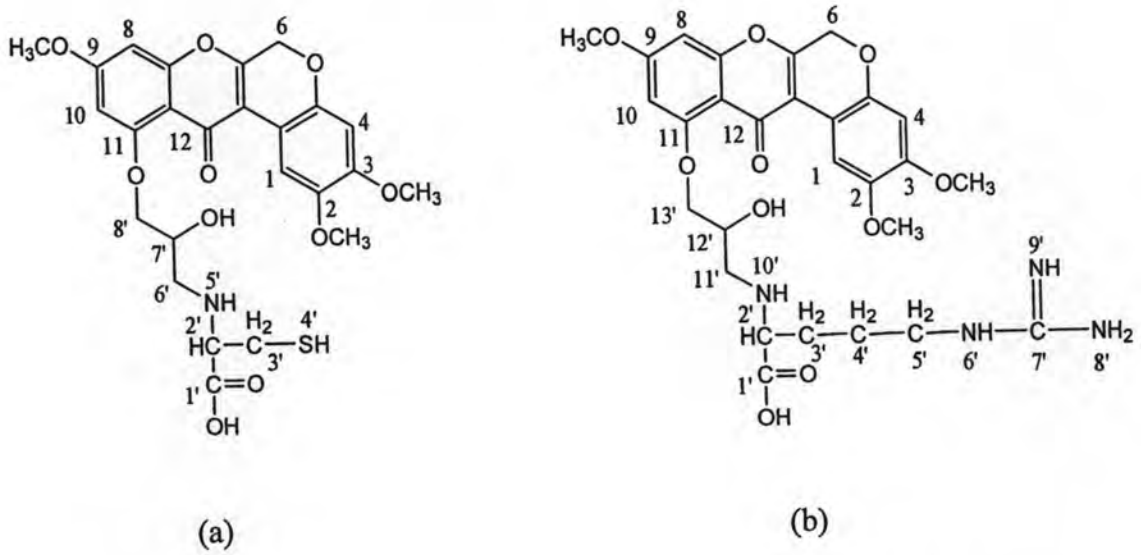

(a) (b)

Fig. 31 The chemical structures of compound (a) **A4**, (b) **A5**

As a result, **A4** and **A5** have the same planar structure. **A4** was inactive in three cell lines. Whereas **A5** showed the most potential cytotoxic activity in KB cell line with the IC_{50} value of 1.45 μg/ml and moderated the cytotoxic activity in MCF7 cell line with the IC_{50} value of 38.45 μg/ml but had inactive in NCI-H187 cell line. There are amino groups in the long side chain of **A5**; it can help to increase its cytotoxicity.

3.5.2 6-deoxyclitoriacetal – pyrimidine base analogues

In order to study the effect of pyrimidine base functional groups on cytotoxicity, three pyrimidine bases were chosen to synthesize with 6-deoxyclitoriacetal; namely cytosine, thymine and uracil. The compound **B** is the tosylate derivative of 6-deoxyclitoriacetal. Compounds **B1** to **B3** are the replacement products of the tosylate derivative with pyrimidine base as given above. All compounds were tested for cytotoxicity against KB (Human mouth carcinoma), MCF7 (Breast cancer) and NCL-H187 (Human small lung cancer) cell lines. The cytotoxic activities of each compounds were indicated as follows.

Compound **B** (Fig. 32b) has tosylate group at C11 of **1**. The side chain has toluene-4-sulfonic acid which is composed of two carbonyl groups. It adopts a bent shape at C6a-C12a. This compound exhibited very strong cytotoxicity against two cancer cell lines. **B** was very active against KB cell line with the IC_{50} value of 0.017 μg/ml and against NCI-H187 cell line with the IC_{50} value of 0.018 μg/ml. Unfortunately, it was inactive against MCF7 cell line.

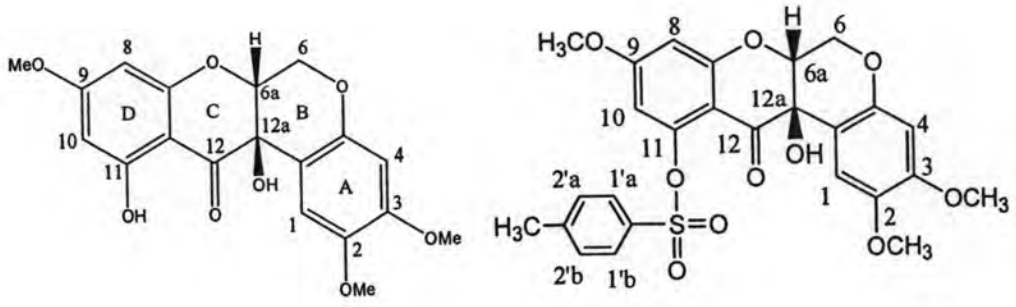

(a) (b)

Fig. 32 The chemical structures of compound (a) **1**, (b) **B**

Compound **B1** (Fig. 33a) was synthesized by adding the pyrimidine base, cytosine, to replace the tosylate group at C11 of **1**. The structure has a double bond at C6a-C12a. Therefore, it adopts only a planar structure. This compound exhibited moderate cytotoxicity against two cancer cell lines; KB cell line with the IC_{50} value of

18.65 μg/ml and against NCI-H187 cell line with the IC_{50} value of 11.61 μg/ml but inactive against MCF7 cell line.

Compound **B2** (Fig. 33b) was synthesized by adding the pyrimidine base, thymine, instead the tosylate group at C11 of **1**. The structure at C6a-C12a position was similar to that of **B1.** Therefore, it also adopts a planar structure. This compound exhibited moderate cytotoxicity against two cancer cell lines; KB cell line with the IC_{50} value of 25.39 μg/ml and NCI-H187 cell line with the IC_{50} value of 11.61 μg/ml. However, inactive against MCF7 cell line.

Compound **B3** (Fig. 33c) was synthesized by adding the pyrimidine base, uracil, instead the tosylate group at C11 of **1**. It also has a planar structure at C6a-C12a position which is similar to that of **B1** and **B2**. **B3** has better cytotoxicity than **B1** and **B2**. It exhibited strong cytotoxicity against KB and NCI-H187 cancer cell lines with the IC_{50} value of 1.45 and 0.255 μg/ml, respectively.

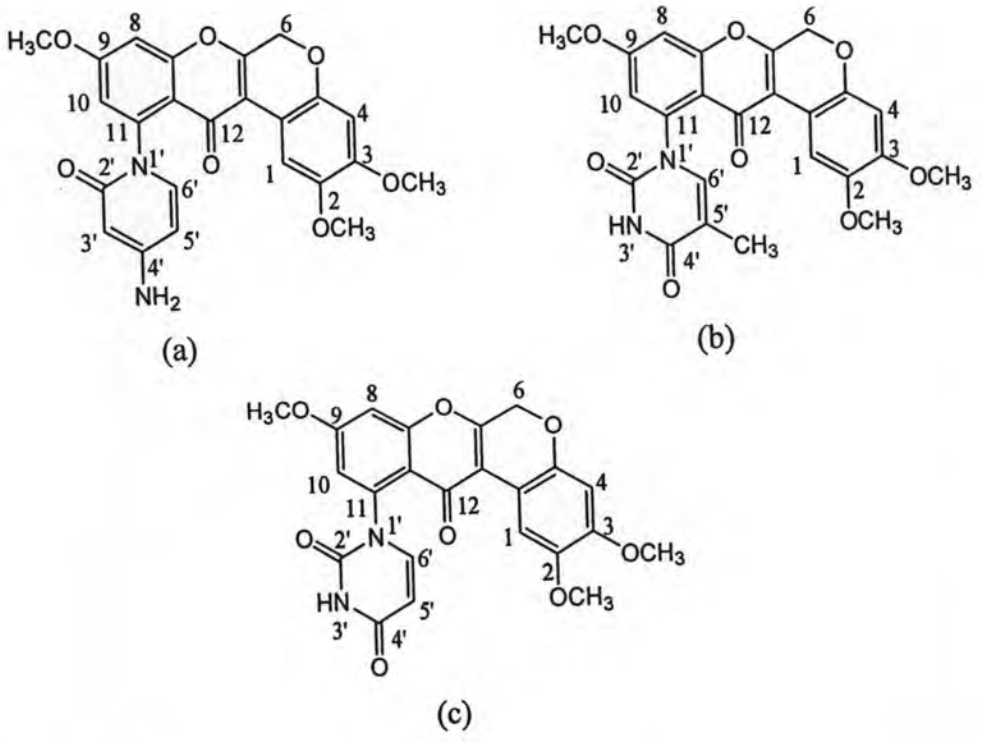

Fig. 33 The chemical structures of compound (a) **B1**, (b) **B2**, (c) **B3**

As a result, **B** showed the most potential cytotoxic activity against KB and NCI-H187 cell lines with the IC_{50} value of 0.017 and 0.018 μg/ml, respectively. This is very possibly because the molecule adopts a bent shape and bears two carbonyl

groups at C11-position. They can increase the stability of the substance-DNA complex by forming strongly hydrogen bonds with DNA. Whereas, **B1** to **B3** was planar structure, they had different cytotoxicities against KB and NCI-H187 cell lines, but showed the same activities in MCF7 and inactive against MCF7 cell lines. For KB cancer cell line, **B3** showed more potential cytotoxic activity than **B1** and **B2**. Since, **B3** has the nitrogen atoms and two carbonyl groups in heterocyclic compounds; they can help to stabilize the DNA complex through the forming hydrogen bonds with DNA. However, **B1** was more active than **B2** in KB cell line because **B1** has the carbonyl group and the amino group, while **B2** presented the methyl group leading to the steric effect. This might disturb the binding of molecule with the base pair in DNA. In addition, the cytotoxic activities of **B1** and **B2** showed the comparative cytotoxic activities in NCI-H187, while **B3** showed the good cytotoxic activity against this cancer cell line.

3.5.3 6-deoxyclitoriacetal – aromatic carboxylic analogues

In order to study the effect of functional group on aromatic carboxylic compound to cytotoxicity, five aromatic carboxylic compounds were chosen to be synthesized with 6-deoxyclitoriacetal namely, 4-*tert*-butylbenzoic acid, benzoic acid, 4-chlorobenzoic acid, 4-hydroxybenzoic acid and 4-aminobenzoic acid. Compounds **C** to **G** are the products of the reaction. All compounds were tested cytotoxicity against KB (Human mouth carcinoma), MCF7 (Breast cancer) and NCL-H187 (Human small lung cancer) cell lines.The cytotoxic activities detail of each compounds were demonstrated as follows.

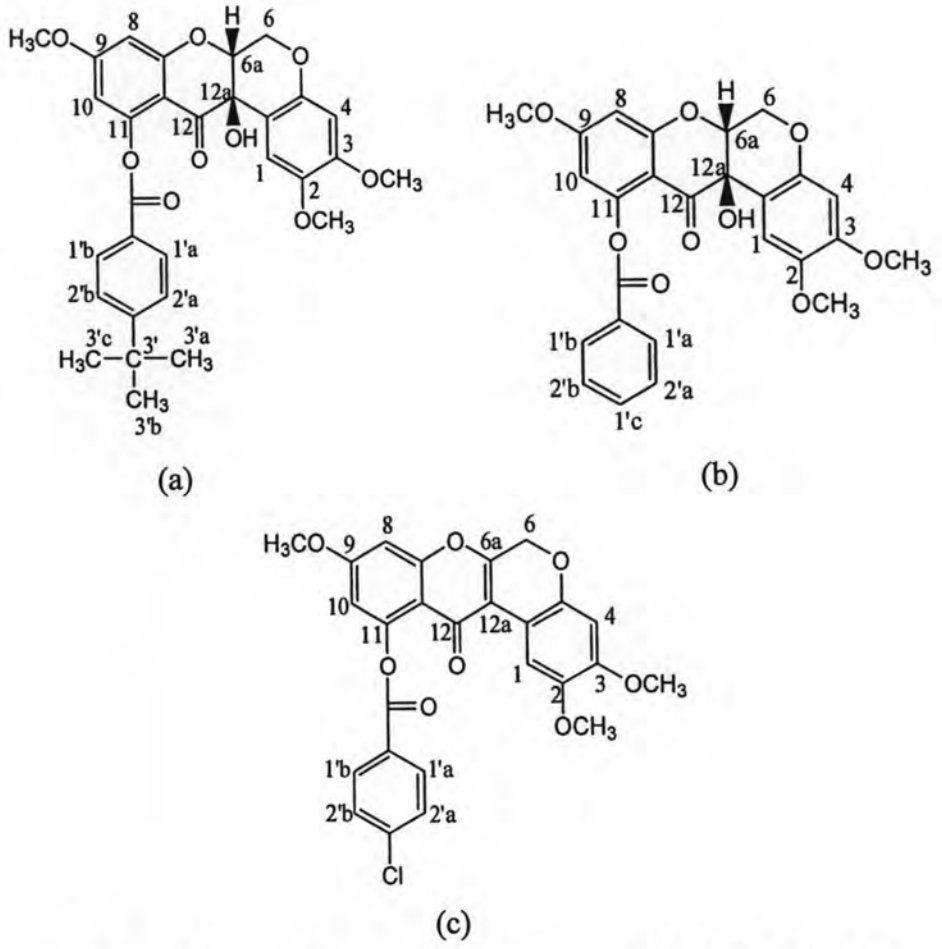

Fig. 34 Chemical structures of compound (a) **C**, (b) **D**, (c) **E**

Compound **C** (Fig. 34a) was the carbonic acid phenyl ester, 4-*tert*-butylbenzoic acid, at C11 of **1**. The structure adopts a bent shape at C6a-C12a. **C** was inactive against KB, MCF7 and NCI-H187, respectively.

Compound **D** (Fig. 34b) was the carbonic acid phenyl ester, benzoic acid, at C11 of **1**. It has also the same bent shape structure as **C**. Compound **D** showed weak cytotoxicity against KB cell line with the IC_{50} value of 40.21 μg/ml while it exhibited moderate cytotoxicity against NCI-H187 cell line with the IC_{50} value of 22.50 μg/ml. It was inactive in MCF7 cancer cell line.

Compound **E** (Fig. 34c) was added the carbonic acid phenyl ester, 4-chlorobenzoic acid, at C11 of **1**. It adopts a planar structure. Compound **E** showed weak cytotoxicity against KB cell line with the IC_{50} value of 47.83 μg/ml while it exhibited moderate cytotoxicity against NCI-H187 cell line with the IC_{50} value of 22.29 μg/ml. It was inactive in MCF7 cancer cell line.

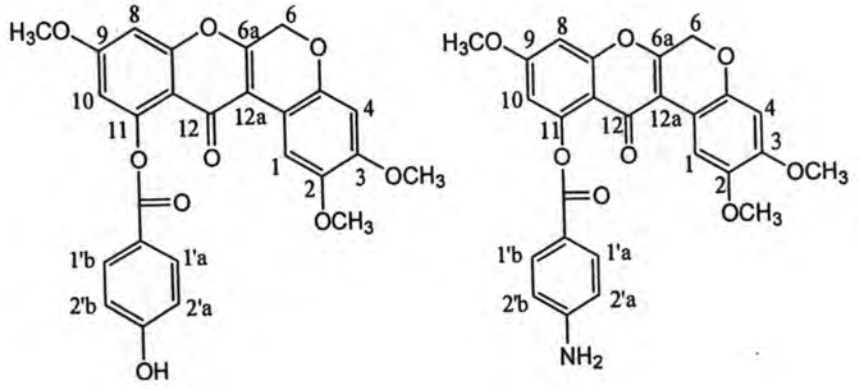

(a) (b)

Fig. 35 The chemical structures of compound (a) **F**, (b) **G**

Compound **F** (Fig. 35a) was added the carbonic acid phenyl ester, 4-hydroxybenzoic acid, at C11 of **1**. It has also a planar structure. Compound **F** showed moderate cytotoxicity against KB and NCI-H187 cancer cell lines with the IC_{50} value of 32.06 and 19.13 μg/ml, respectively. It was inactive in MCF7 cancer cell line.

Compound **G** (Fig. 35b) was added the carbonic acid phenyl ester, 4-aminobenzoic acid, at C11 of **1**. It adopts the same planar structure as **E** and **F**. Interestingly, **G** showed strong cytotoxicity against KB and NCI-H187 cancer cell lines with the IC_{50} value of 2.64 and 8.28 μg/ml, respectively. However, it was inactive in MCF7 cancer cell line.

As a result, compound **C** to **G** was inactive against MCF-7, but they showed differently cytotoxic activities in KB and NCI-H187 cancer cell lines. Compound **C** was inactive in three cell lines because of the steric effect at the position of 4-*tert*-butyl group. However, the other compounds' cytotoxic activities were correlated with the functional group of carbonic acid. In KB and NCI-H187 cell lines, the cytotoxic activities of **C** to **G** were corresponding with the functional group that forming the hydrogen bonding with DNA base pairs. Compound **D** has no functional group; it showed the IC_{50} value of in KB and NCI-H187 cell lines at 40.21 and 22.50 μg/ml, respectively. While **E** has chloride as the functional group but it showed weakly cytotoxic activities with the IC_{50} value of 47.83 and 27.29 μg/ml in KB and NCI-H187, respectively because of no forming hydrogen with DNA base pairs.

Interestingly, compound **F** has hydroxyl group as functional group, it was active against KB and NCI-H187 with the IC_{50} value of 32.06 and 19.13 μg/ml, respectively. These values were higher than that of **D** and **E**. All of compounds in this group, compound **G** showed the most potential cytotoxic activities against KB and NCI-H187 cell lines with the IC_{50} value of 2.64 and 8.28 μg/ml, respectively. The NH_2 group in compound **G** also increases the stability of the complex through forming hydrogen bonds with DNA. Based on such reasons the functional group in the compounds plays an important role in exhibiting an anticancer activity.

Interestingly, several compounds were inactive against MCF7 (breast cancer cell line). MCF7 cell line is the estrogen receptor-positive cell line. It is used to a prominent model system for the study of breast cancer. Despite the fact that many tumors initially respond to chemotherapy, breast cancer cells can subsequently survive and gain resistance to the treatment. Tamoxifen (Fig. 32) is the anticancer drug used to treat the breast cancer [59]. Therefore, several compounds were inactive against MCF7 probably because this cell line was easy to resistant with many compounds. Moreover, the competitive compounds to be a breast anticancer should have a pharmacophore similar to estrogen receptor. Therefore, it can be noticed that our tested compounds has different structure to Tamoxifen, which is an anticancer drug which specific with the breast cancer, resulting in inactive activity for MCF7 cell lines.

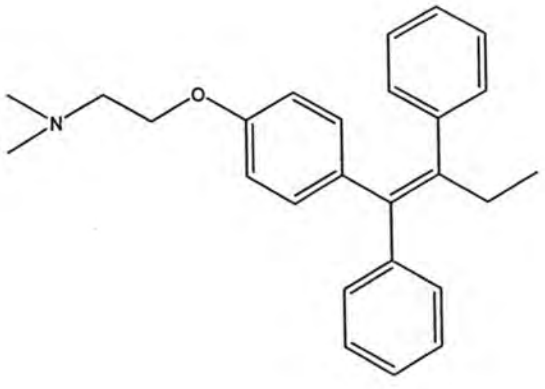

Fig. 36 The chemical structure of Tamoxifen

3.6 Effect of 1, 2 and analogues of 1 on the Relaxation Activity of Topoisomerase II

Topoisomerase II is an important nuclear enzyme controlling DNA topology through catalysis of a breakage of double-stranded DNA, allowing for the passage of double-stranded DNA followed by resealing the DNA. Relaxation of DNA supercoils by topoisomerase II is considered crucial for DNA replication and transcription [60]. To further elucidate cytotoxicity of 6-deoxyclitoriacetal, stemonal and 6-deoxyclitoriacetal analogues (**A1** to **A5**),, the relaxation of supercoiled plasmid pBR322 DNA was evaluated. Topoisomerase II relaxation assay was conducted using human topoisomerase II (Amersham). Etoposide are selective topoisomerase II inhibitors being used as a positive control. The data were analyzed and calculated with Syngene software for the % inhibition. The results of inhibition were described in Table 22 and Fig. 37.

Table 22 Topoisomerase II inhibition rate (%) and IC_{50} (μg/ml) of 6-deoxyclitoriacetal, stemonal and 6-deoxyclitoriacetal analogues, **A1** to **A5**

Compound	Relaxation activity for Topoisomerase II % Inhibition	IC_{50} (μg/ml)		
		KB	MCF7	NCl-H187
Etoposide	68.94	-	-	-
stemonal	37.25	Inactive	Inactive	Inactive
6-deoxyclitoacetal	73.51	0.08	0.26	0.04
A1	50.10	23.22	Inactive	20.74
A2	35.60	35.54	25.61	3.31
A3	31.50	5.05	18.67	6.01
A4	30.20	Inactive	Inactive	Inactive
A5	39.50	1.45	38.45	Inactive

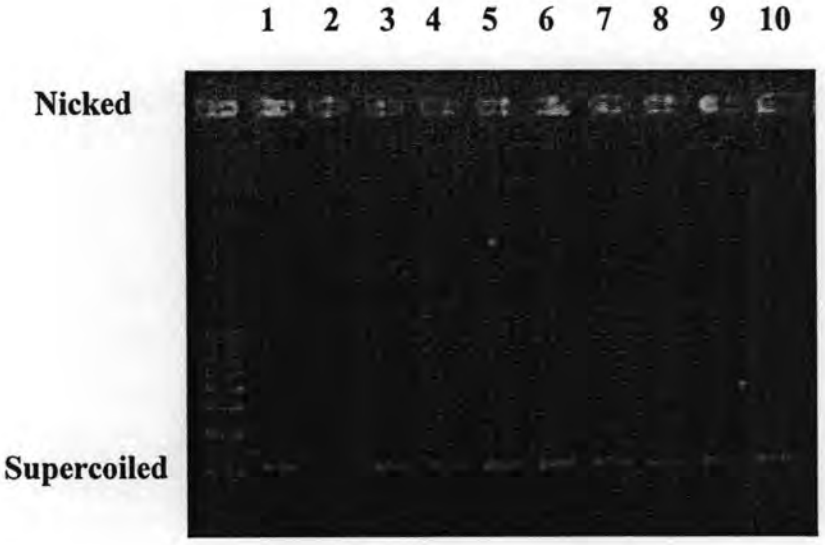

Fig. 37 Topoisomerase II inhibition test of compounds.. Lane 1: pBR322 only, Lane 2: Topo II + pBR322, Lane 3: etoposide, 100 μM, Lane 4: stemonal at concentration of 100 μM, Lane 5: 6-deoxyclitoriacetal at concentration of 100 μM, Lane 6-10: **A1** to **A5** at concentration of 100 μM, respectively.

The inhibitory activity of all compounds on the activity of topoisomerase II was assayed. Among these compounds, the inhibition rate in the presence of 100 μg/ml of 6-deoxyclitoriacetal and 100 μg/ml etoposide were 73.51 % and 68.94 %, respectively. The topoisomerase II inhibition of 6-deoxyclitoriacetal was superior over etoposide used as a reference drug. For **A1** to **A5** at a concentration of 100 μg/ml showed to moderately inhibit the conversion of DNA to the supercoiled form (Table 22). The stemonal showed 37.25 % inhibition rate against topoisomerase II action at 100 μg/ml. The inhibition rate in the presence of 100 μg/ml of **A1–A5** was 50.10, 35.60, 31.50, 30.20 and 39.50 %, respectively, compared to 68.94 % of etoposide. It can be concluded that the 6-deoxyclitoriacetal was more potent topoisomerase II inhibitor than the etoposide, stemonal and its analogues (**A1-A5**).

Based on the 6-deoxyclitoriacetal analogues, **A1-A5** was evaluated for the catalytic activity of Topoisomerase II. In this case, compounds **A1** had the strongest inhibitory activity, giving 50.10 % inhibition at 100 μg/ml, and were comparable with the antitumor agent etoposide (68.94 % inhibition). Compound **A2** to **A5** also caused moderate inhibition of 35.60%, 31.50%, 30.20%, and 39.50%, respectively.

Although, 6-deoxyclitoriacetal, stemonal and **A1-A5** had the different cytotoxicity, they showed the relatively selective inhibitory against topoisomerase II. Interestingly, all compounds shared the same planar structure so they can inhibit topoisomerase II. This might be one of the factors for the catalytic of inhibitory against topoisomerase II.

The obvious correlation between the cytotoxicity and the inhibitory activity of topoisomerase II was observed only in 6-deoxyclitoriacetal. The 6-deoxyclitoriacetal had good cytotoxic activities, compared to doxorubicin and ellipticine, with IC_{50} at 0.08, 0.26 and 0.04 μg/ml in KB, MCF7 and NCI-H187, respectively. These cytotoxic activities were correlated with the high inhibitory topoisomerase II, giving 75.22 % inhibition compared to etoposide (68.94 % inhibition).

However, no obvious correlation was observed between the cytotoxicity and the inhibitory activity of topoisomerase II in stemonal and **A1-A5**. Especially, stemonal and **A4** were inactive in three cancer cell lines, KB, MCF7 and NCI-H187, respectively, but showed the moderate inhibition of topoisomerase II.

Interestingly, the presence of a substituent at C11 in **A1** to **A5** reduced the inhibition of topoisomerase II. This is probably due to the steric hindrance that might affect topoisomerase II inhibition.